NFN - Nationales Forschungsnetzwerk

Geometry + Simulation

http://www.gs.jku.at

Isogeometric Analysis with Geometrically Continuous Functions on Multi-Patch Geometries

Mario Kapl, Florian Buchegger, Michel Bercovier, Bert Jüttler

G+S Report No. 35

August 2015

Der Wissenschaftsfonds.

JOHANNES KEPLER UNIVERSITY LINZ

Isogeometric Analysis with Geometrically Continuous Functions on Multi-Patch Geometries

Mario Kapl[a], Florian Buchegger[a], Michel Bercovier[b], Bert Jüttler[a,*]

[a] *Johannes Kepler University, Linz, Austria*
[b] *The Hebrew University of Jerusalem, Israel*

Abstract

We present a method for generating a basis of the space of bicubic and biquartic C^1-smooth geometrically continuous isogeometric functions on bilinear multi-patch domains $\Omega \subset \mathbb{R}^2$. The resulting basis functions are constructed from C^1-smooth geometrically continuous isogeometric functions on bilinearly parameterized two patch domains (cf. [10]) and are described by explicit formulas for the Bézier coefficients of their spline segments. These C^1-smooth isogeometric functions possess potential for applications in isogeometric analysis, which is demonstrated by several examples (e.g. solving the biharmonic equation). The numerical results indicate optimal rates of convergence.

Keywords: Isogeometric Analysis, C^1-smooth isogeometric functions, geometrically continuous isogeometric functions, multi-patch domain, biharmonic equation

1. Introduction

Isogeometric Analysis (IgA) is a promising framework for performing numerical simulation, which uses the same (rational) spline function space for representing the geometry of the physical domain and describing the solution space [4, 9]. One possibility in IgA to deal with domains of general topology is the use of multi-patch parameterizations. Several methods for coupling the single patches exist, e.g. [2, 3, 7, 12, 13, 16, 19], but most of these techniques do not provide globally C^1-smooth functions.

A recent strategy to overcome this limitation is the use of the concept of geometric continuity [17]. This concepts represents a well known approach in Computer Aided Geometric Design for generating smooth multi-patch surfaces possessing extraordinary vertices [5, 8]. The construction of C^1-smooth functions (or even functions with higher smoothness) is based on the observation – which has been formalized firstly by Groisser and Peters [6] – that the C^s-smoothness of an isogeometric function is equivalent to the geometric smoothness of order s (G^s-smoothness) of its graph surface, where s is a positive integer. This fact

*Corresponding author
Email addresses: mario.kapl@jku.at (Mario Kapl), florian.buchegger@jku.at (Florian Buchegger), berco@cs.huji.ac.il (Michel Bercovier), bert.juettler@jku.at (Bert Jüttler)

motivated us to denote the C^s-smooth functions on a multi-patch domain as *C^s-smooth geometrically continuous isogeometric functions* [10].

For the case $s = 1$, two different strategies following the concept of geometric smoothness have been explored. One approach derives the C^1-smooth functions from methods for constructing G^1-smooth multi-patch surfaces. Examples are the techniques [11, 14, 15], which are based on different G^1-smooth multi-patch spline surface constructions, or the method [18], which generates the C^1-smooth functions by means of a T-spline representation (cf. [20, 21]). In contrast, the second approach generates a basis of the entire space of C^1-smooth functions on a particular class of multi-patch geometries, cf. [1, 10]. E.g. in [10], the space of bicubic and biquartic C^1-smooth geometrically continuous isogeometric functions on bilinearly parameterized two-patch domains has been analyzed. Furthermore, a simple framework for the construction of a basis for this space has been developed.

The present work extends the results of [10] to bilinearly parameterized multi-patch domains. Analogous to [10], the numerical experiments indicate that the space of C^1-smooth geometrically continuous isogeometric functions provides the full approximation power of splines for these multi-patch domains. Among other examples we numerically solve the biharmonic equation on different bilinear multi-patch geometries, where the isogeometric analysis is simplified by using the C^1-smoothness of the discretization space.

The paper is organized as follows. Section 2 describes the class of bilinearly parameterized multi-patch domains $\Omega \subset \mathbb{R}^2$, which is considered throughout this paper. In addition, we present the concept of bicubic and biquartic C^1-smooth geometrically continuous isogeometric functions, which was introduced for a more general setting in [10].

The explicit construction of a basis of the space of C^1-smooth geometrically continuous isogeometric functions defined on bilinearly parameterized *two*-patch domains for biquartic functions from [10] is recalled in Section 3. In addition we present a similar new construction for bicubic functions. Moreover, we propose a different choice of the basis functions in the vicinity of patch vertices of valence $m \geq 3$, since this will be advantageous for analyzing the full multi-patch case. Explicit formulas for the Bézier coefficients of the spline segments of all functions are specified in Appendix A.

We then use the different functions for the two patch case to generate a basis of the space of C^1-smooth geometrically continuous isogeometric functions on bilinear multi-patch domains in Section 4. The dimension of the resulting space of the C^1-smooth isogeometric functions is also analyzed. Finally, Section 5 shows several examples that demonstrate the potential of our construction for isogeometric analysis. More precisely, we use C^1-smooth bicubic and biquartic functions for performing L^2-approximation and for solving Poisson's equation and the biharmonic equations on different multi-patch domains. The numerical results indicate optimal rates of convergence.

2. Preliminaries

The notion of C^s-smooth geometrically continuous isogeometric functions on general multi-patch domains was introduced in [10, Section 2]. In this section, we first present the particular class of bilinear multi-patch domains $\Omega \subset \mathbb{R}^2$, which will be considered throughout the paper. Then we recall the concept of geometrically continuous functions for $s = 1$.

2.1. Bilinearly parameterized multi-patch domains

For a given degree $d \in \{3, 4\}$ and a number of inner knots k satisfying $k \geq 5 - d$, we denote with $\mathcal{S}^d_{k,p}$ the tensor-product spline space of degree (d, d), which is defined on $[0, 1]^2$ by choosing k uniform inner knots of multiplicity $p \geq 0$ in both parameter directions. We consider a computational domain

$$\Omega = \bigcup_{\ell=1}^{n} \Omega^{(\ell)} \subset \mathbb{R}^2$$

which is the union of n quadrilateral patches $\Omega^{(\ell)}$, $\ell \in \{1, \ldots, n\}$. Each patch is the image $\Omega^{(\ell)} = \boldsymbol{G}^{(\ell)}([0, 1]^2)$ of the unit square under a bijective, regular geometry mapping

$$\boldsymbol{G}^{(\ell)} \in \mathcal{S}^d_{k,d-1} \times \mathcal{S}^d_{k,d-1} : [0, 1]^2 \to \mathbb{R}^2,\ \boldsymbol{\xi}^{(\ell)} = (\xi_1^{(\ell)}, \xi_2^{(\ell)}) \mapsto (G_1^{(\ell)}, G_2^{(\ell)}) = \boldsymbol{G}^{(\ell)}(\boldsymbol{\xi}^{(\ell)}).$$

Each geometry mapping $\boldsymbol{G}^{(\ell)}$ is represented in the form

$$\boldsymbol{G}^{(\ell)}(\boldsymbol{\xi}^{(\ell)}) = \sum_{\boldsymbol{i} \in \hat{I}} \widehat{\boldsymbol{d}}_{\boldsymbol{i}}^{(\ell)} \widehat{\psi}_{\boldsymbol{i}}(\boldsymbol{\xi}^{(\ell)}),$$

with spline control points $\widehat{\boldsymbol{d}}_{\boldsymbol{i}}^{(\ell)} \in \mathbb{R}^2$ and tensor-product B-splines $\widehat{\psi}_{\boldsymbol{i}}$ spanning the spline space $\mathcal{S}^d_{k,d-1}$ where $\hat{I} = \{(i_1, i_2) \mid 0 \leq i_j \leq d + kd - k, j = 1, 2\}$ is the index set. Each geometry mapping $\boldsymbol{G}^{(\ell)}$ has a Bézier representation

$$\boldsymbol{G}^{(\ell)}(\boldsymbol{\xi}^{(\ell)}) = \sum_{\boldsymbol{i} \in \tilde{I}} \widetilde{\boldsymbol{d}}_{\boldsymbol{i}}^{(\ell)} \widetilde{\psi}_{\boldsymbol{i}}(\boldsymbol{\xi}^{(\ell)}),$$

where $\tilde{I} = \{(i_1, i_2) \mid 0 \leq i_j \leq d + k + kd, j = 1, 2\}$ is the index set, $\widetilde{\boldsymbol{d}}_{\boldsymbol{i}}^{(\ell)} \in \mathbb{R}^2$ are the Bézier control points and $\widetilde{\psi}_{\boldsymbol{i}}$ are the tensor-product B-splines of the space $\mathcal{S}^d_{k,d+1}$. Let I be the index space

$$I = \bigcup_{\ell \in \{1,\ldots,n\}} \{\ell\} \times \tilde{I}.$$

For a common interface $\boldsymbol{e}$ of two neighboring spline patches $\boldsymbol{G}^{(\ell)}$, we denote by $I_{\boldsymbol{e}} \subseteq I$ the index space

$$I_{\boldsymbol{e}} = \{(\ell, \boldsymbol{i}) \in I | \widetilde{\boldsymbol{d}}_{\boldsymbol{i}}^{(l)} \text{ is Bézier control point of the interface } \boldsymbol{e} \text{ or of one} \\ \text{of the two neighboring columns of control points on each side of } \boldsymbol{e}.\}$$

Throughout the paper, we will make the following additional assumptions concerning the multi-patch domain Ω:

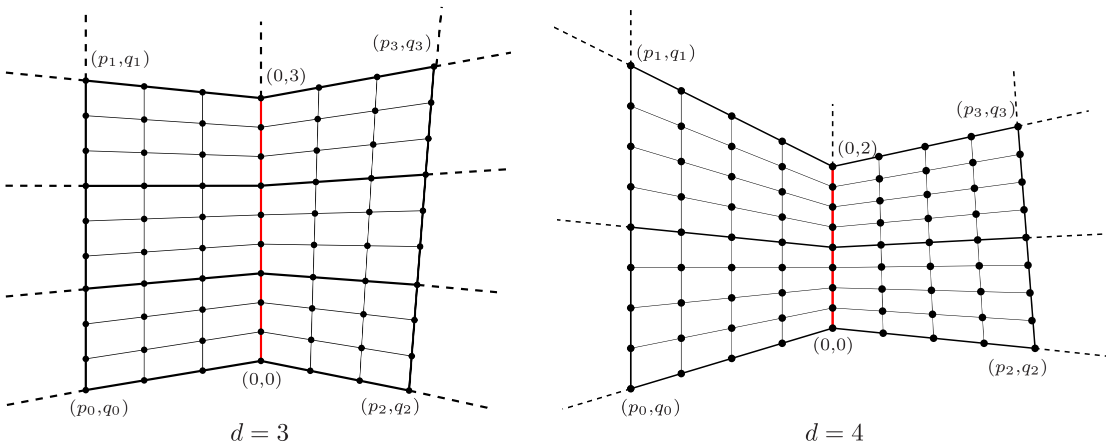

Figure 1: The local geometry of the first three (for $d=3$) and first two (for $d=4$) pairs of neighboring spline segments of a two-patch domain is determined by the 6 patch vertices $(0,0)$, $(0,3)/(0,2)$ and (p_i,q_i), $i=0,\ldots,3$.

I. All geometry mappings $\boldsymbol{G}^{(\ell)}$, $\ell\in\{1,\ldots,n\}$, are also defined and regular on a neighborhood of $[0,1]^2$ and the interiors of all patches $\Omega^{(\ell)}$, $\ell\in\{1,\ldots,n\}$, are mutually disjoint, i.e.

$$\boldsymbol{G}^{(\ell)}((0,1)^2)\cap\boldsymbol{G}^{(\ell')}((0,1)^2)=\emptyset$$

for $\ell,\ell'\in\{1,\ldots,n\}$ with $\ell\neq\ell'$.

II. Two neighboring patches $\Omega^{(\ell)}$ and $\Omega^{(\ell')}$, $\ell,\ell'\in\{1,\ldots,n\}$ with $\ell\neq\ell'$, always share the whole common edge, i.e. the multi-patch domain Ω has no T-joints. We denote the resulting two-patch domain $\Omega^{(\ell)}\cup\Omega^{(\ell')}$ by $\Omega^{(\ell\ell')}$ and denote their common interface by $\boldsymbol{e}^{(\ell\ell')}$.

III. All two-patch domains $\Omega^{(\ell\ell')}$ of two neighboring patches $\Omega^{(\ell)}$ and $\Omega^{(\ell')}$, $\ell,\ell'\in\{1,\ldots,n\}$ with $\ell\neq\ell'$, satisfy the so-called genericity condition (cf. [10, Eq. (10)]). Assume that the two-patch domain $\Omega^{(\ell\ell')}$ is determined by the 6 patch vertices $(0,0)$, $(0,1)$ and (p_i,q_i), $i=0,\ldots,3$, see [10, Fig. 2], and that the corresponding geometry mappings $\boldsymbol{G}^{(\ell)}$ and $\boldsymbol{G}^{(\ell')}$ satisfy $\boldsymbol{G}^{(\ell)}(1,\xi_2)=\boldsymbol{G}^{(\ell')}(0,\xi_2)$. Then the condition

$$p_1p_2\neq p_0p_3$$

is fulfilled, and for $j\in\{1,\ldots,k\}$ the 3 different Bézier control points $\widetilde{\boldsymbol{d}}_{\boldsymbol{i}}^{(\ell)}$ of the set

$$\{\widetilde{\boldsymbol{d}}_{\boldsymbol{i}}^{(p)}|(p,\boldsymbol{i})\in I_{\boldsymbol{e}^{(\ell\ell')}} \text{ and } \boldsymbol{d}_{\boldsymbol{i}}^{(p)} \text{ is a Bézier control point that corresponds to the } d+2 \text{ knots } (\tfrac{j-1}{k+1},\tfrac{j}{k+1},\ldots,\tfrac{j}{k+1}) \text{ in } \xi_1^{(\ell)}\text{-direction.}\}$$

are not collinear.

IV. We make the following technical assumption for each boundary vertex of valence $m=3$ of the multi-patch domain Ω. After transforming the coordinates of the vertices of the first $6-d$ pairs of spline segments into the canonical coordinate system shown in Fig. 1, where $(0,0)$ is the corresponding boundary vertex, the coordinates satisfy the condition

$$p_0((5-d)q_2+q_3-(6-d)) \neq ((5-d)p_2+p_3)(q_0-1).$$

This condition means that the three points $(0,1)$, (p_0,q_0) and $(\frac{(5-d)p_2+p_3}{6-d}, \frac{(5-d)q_2+q_3}{6-d})$ are not collinear.

V. We make the following technical assumption for each inner vertex of arbitrary valence (i.e. $m \geq 3$) or boundary vertex of valence $m \geq 4$ of the multi-patch domain Ω. After transforming the coordinates of the vertices of the first $6-d$ pairs of spline segments into the canonical coordinate system shown in Fig. 1, where $(0,0)$ is the corresponding vertex, the coordinates satisfy the two conditions

$$p_0 q_2 \neq p_2 q_0$$

and

$$p_0(1-q_2) \neq p_2(1-q_0).$$

The first condition means that the three points $(0,0)$, (p_0,q_0) and (p_2,q_2) are not collinear, and the second condition means that the three points $(0,1)$, (p_0,q_0) and (p_2,q_2) are not collinear.

Examples of such multi-patch domains are shown in Fig. 11 (first row).

2.2. Space of C^1-smooth functions on bilinear multi-patch geometries

The space $\widetilde{V}$ of isogeometric functions on a multi-patch domain Ω is given by

$$\widetilde{V} = \left\{ v \in \Omega : v|_{\Omega^{(\ell)}} \in \mathcal{S}^d_{k,d-1} \circ (\boldsymbol{G}^{(\ell)})^{-1} \text{ for all } \ell \in \{1,\dots,n\} \right\}.$$

An isogeometric function $w \in \widetilde{V}$ is represented on each patch $\Omega^{(\ell)}$, $\ell \in \{1,\dots,n\}$, by

$$(w|_{\Omega^{(\ell)}})(\boldsymbol{x}) = w^{(\ell)}(\boldsymbol{x}) = \left(W^{(\ell)} \circ (\boldsymbol{G}^{(\ell)})^{-1} \right)(\boldsymbol{x}), \quad \boldsymbol{x} \in \Omega^{(\ell)},$$

with $W^{(\ell)} \in \mathcal{S}^d_{k,d-1}$, and the associated graph surface $\boldsymbol{F}^{(\ell)}$ of $w^{(\ell)}$ is given by

$$\boldsymbol{F}^{(\ell)}(\boldsymbol{\xi}^{(\ell)}) = \Big(\underbrace{G_1^{(\ell)}(\boldsymbol{\xi}^{(\ell)}), G_2^{(\ell)}(\boldsymbol{\xi}^{(\ell)})}_{=\boldsymbol{G}^{(\ell)}(\boldsymbol{\xi}^{(\ell)})}, W^{(\ell)}(\boldsymbol{\xi}^{(\ell)}) \Big)^T.$$

Each function $W^{(\ell)}$, $\ell \in \{1,\dots,n\}$, has a local spline representation

$$W^{(\ell)}(\boldsymbol{\xi}^{(\ell)}) = \sum_{\boldsymbol{i} \in \hat{I}} b_{\boldsymbol{i}}^{(\ell)} \widehat{\psi}_{\boldsymbol{i}}(\boldsymbol{\xi}^{(\ell)}),$$

with $b_{\boldsymbol{i}}^{(\ell)} \in \mathbb{R}$. Consequently, $W^{(\ell)}$ has also a local Bézier representation

$$W^{(\ell)}(\boldsymbol{\xi}^{(\ell)}) = \sum_{\boldsymbol{i}\in\tilde{I}} a_{\boldsymbol{i}}^{(\ell)} \widetilde{\psi}_{\boldsymbol{i}}(\boldsymbol{\xi}^{(\ell)}),$$

with $a_{\boldsymbol{i}}^{(\ell)} \in \mathbb{R}$. For a function $w \in \widetilde{V}$, we denote by $\mathrm{supp}_{\mathrm{BB}}(w) \subseteq I$ the support of w in the Bézier coefficient space, i.e.

$$\mathrm{supp}_{\mathrm{BB}}(w) = \{(\ell, \boldsymbol{i}) \in I | a_{\boldsymbol{i}}^{(\ell)} \text{ is Bézier coefficient of } W^{(\ell)} \text{ with } a_{\boldsymbol{i}}^{(\ell)} \neq 0\}.$$

In the following, we are interested in the space $V = \widetilde{V} \cap C^1(\Omega)$, i.e.

$$V = \left\{ v \in C^1(\Omega) : v|_{\Omega^{(\ell)}} \in \mathcal{S}_{k,d-1}^{d} \circ (\boldsymbol{G}^{(\ell)})^{-1} \text{ for all } \ell \in \{1, \ldots, n\} \right\},$$

that contains the globally C^1-smooth isogeometric functions defined on the multi-patch domain Ω. According to [10, Theorem 1] an isogeometric function $w \in \widetilde{V}$ belong to the space V if and only if for all neighboring patches $\Omega^{(\ell)}$ and $\Omega^{(\ell')}$, $\ell, \ell' \in \{1, \ldots, n\}$ with $\ell \neq \ell'$, the associated graph surfaces $\boldsymbol{F}^{(\ell)}$ and $\boldsymbol{F}^{(\ell')}$ are G^1-smooth along the common interface $\boldsymbol{e}^{(\ell\ell')}$. This equivalence of the C^1-smoothness of an isogeometric function and the G^1-smoothness of its graph surfaces is the reason to call the functions $w \in V$ also *C^1-smooth geometrically continuous isogeometric functions.*

As described in [10, Subsection 2.3], by imposing the G^1-smoothness between the graph surfaces of all neighboring patches $\Omega^{(\ell)}$, $\Omega^{(\ell')}$, $\ell, \ell' \in \{1, \ldots, n\}$ with $\ell \neq \ell'$, we obtain linear constraints on the spline coefficients $b_{\boldsymbol{i}}^{(\ell)}$ or on the Bézier coefficients $a_{\boldsymbol{i}}^{(\ell)}$. This can be formulated as a homogeneous linear system

$$\hat{H}\boldsymbol{b} = 0, \quad \boldsymbol{b} = \left(b_{\boldsymbol{i}}^{(\ell)}\right)_{\ell\in\{1,2,\ldots,n\},\boldsymbol{i}\in\hat{I}} \tag{1}$$

or

$$\tilde{H}\boldsymbol{a} = 0, \quad \boldsymbol{a} = \left(a_{\boldsymbol{i}}^{(\ell)}\right)_{(\ell,\boldsymbol{i})\in I}, \tag{2}$$

respectively. Then a basis of the nullspace of $\hat{H}$ or $\tilde{H}$ defines via the spline coefficients $b_{\boldsymbol{i}}^{(\ell)}$ or the Bézier coefficients $a_{\boldsymbol{i}}^{(\ell)}$, respectively, a basis of C^1-smooth geometrically continuous isogeometric functions for the space V.

A construction of a basis of V for bilinearly parameterized two-patch domains is explained in [10, Section 3], where the generated basis consists of two different kinds of functions. In the following section, we will present these two different kinds of basis functions. This provides us a possibility to generate a basis of V for bilinearly parameterized multi-patch domains Ω, see Section 4. Thereby, the basis functions will be generated by means of a suitable choice of the Bézier coefficients $a_{\boldsymbol{i}}^{(\ell)}$.

3. C^1-smooth functions on bilinear two-patch geometries

In this section, we restrict ourselves to two-patch domains $\Omega = \Omega^{(1)} \cup \Omega^{(2)}$ that satisfy Assumptions I-IV. As explained in [10, Section 3], a possible basis of the space V for bilinearly parameterized two-patch domains consists of two different kinds of C^1-smooth geometrically continuous isogeometric basis functions, called basis functions of the first kind and basis functions of the second kind. In this paper, we will refer to these two different kinds of basis functions as *patch basis functions* and *edge basis functions*, respectively. We summarize them, especially with respect to the choice of the corresponding Bézier coefficients $a_{\boldsymbol{i}}^{(\ell)}$. In the case of the edge basis functions, we recall an explicit construction of these functions for $d = 4$ from [10] and present a new similar construction for $d = 3$. In addition, we present for both degrees a further explicit construction of the edge basis functions in the vicinity of the boundary vertices of a common interface. All the presented functions are used in Section 4 to generate C^1-smooth basis functions defined on the bilinear multi-patch domains Ω.

3.1. Patch basis functions

These functions are obtained by composing a tensor-product B-spline function $\widehat{\psi}_{\boldsymbol{i}}$ of one patch $\Omega^{(\ell)}$, that has function values and first partial derivatives equal to zero along a common interface with another patch, with the inverse of the geometry mapping $\boldsymbol{G}^{(\ell)}$, i.e.

$$\boldsymbol{x} \mapsto \begin{cases} (\widehat{\psi}_{\boldsymbol{i}} \circ (\boldsymbol{G}^{(\ell)})^{-1})(\boldsymbol{x}) \text{ if } \mathbf{x} \in \Omega^{(\ell)} \\ 0 \text{ otherwise} \end{cases} \qquad \ell \in \{1, 2\}. \tag{3}$$

The support of each function is contained in only one of the two patches $\Omega^{(1)}$ and $\Omega^{(2)}$. In addition, exactly one spline coefficient $b_{\boldsymbol{i}}^{(\ell)}$ is non-zero, which has the value one. All coefficients $b_{\boldsymbol{i}}^{(\ell)}$ that correspond to the spline control points of the common interface or one of the neighboring columns of the two patches $\boldsymbol{G}^{(1)}$ and $\boldsymbol{G}^{(2)}$ are zero. That means, for each spline control point of the geometry mappings $\boldsymbol{G}^{(1)}$ and $\boldsymbol{G}^{(2)}$, that do not belong to the common interface of the two patches and to the neighboring column of spline control points, we have exactly one patch basis function. Therefore, the number of such functions for a two-patch domain is given by

$$2(d - 1 + k(d - 1))(d + 1 + k(d - 1)).$$

Since the support of the tensor-product function $\widehat{\psi}_{\boldsymbol{i}}$ can be obtained in one, two or four spline segments of the corresponding geometry mapping $\boldsymbol{G}^{(\ell)}$, more than one Bézier coefficient $a_{\boldsymbol{i}}^{(\ell)}$ can be non-zero with $a_{\boldsymbol{i}}^{(\ell)} \in \{\frac{1}{4}, \frac{1}{2}, 1\}$, and these values are independent of the geometry mappings. Analogous to the spline coefficients $b_{\boldsymbol{i}}^{(\ell)}$, all Bézier coefficients $a_{\boldsymbol{i}}^{(\ell)}$ that correspond to the Bézier control points of the common interface or one of the neighboring columns of the corresponding spline segments of $\boldsymbol{G}^{(1)}$ and $\boldsymbol{G}^{(2)}$ have to be zero, i.e. $a_{\boldsymbol{i}}^{(\ell)} = 0$ for $(\ell, \boldsymbol{i}) \in I_{\boldsymbol{e}^{(12)}}$. Fig. 2 and 3 shows all possible supports of a patch basis function w in the Bézier coefficient space (i.e. $\mathrm{supp}_{\mathrm{BB}}(w)$) with their corresponding values of the Bézier coefficients $a_{\boldsymbol{i}}^{(\ell)}$ for $d = 3$ and $d = 4$, respectively.

3.2. Edge basis functions

These functions w possess a support that is contained in both patches $\Omega^{(1)}$ and $\Omega^{(2)}$, where $\mathrm{supp}_{\mathrm{BB}}(w)$ consists only of Bézier coefficients $a_{\boldsymbol{i}}^{(\ell)}$ with $(\ell, \boldsymbol{i}) \in I_{\boldsymbol{e}^{(12)}}$. In contrast to

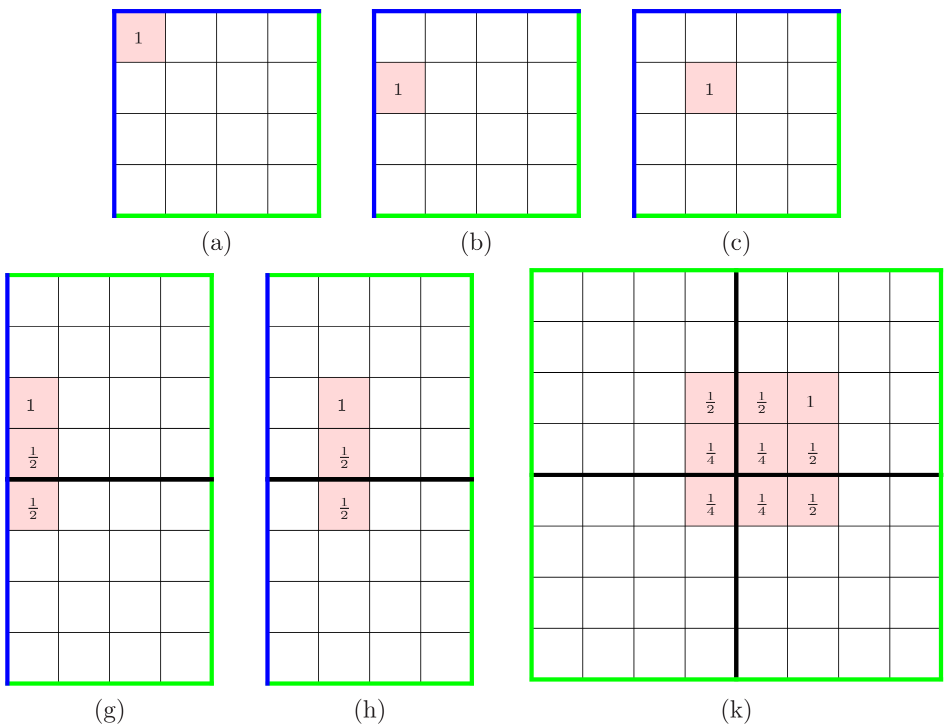

Figure 2: All possible supports $\mathrm{supp}_{\mathrm{BB}}(w)$ (red squares) of the patch basis functions w for $d = 3$ with the corresponding values of the Bézier coefficients $a_{\boldsymbol{i}}^{(\ell)}$ up to symmetries. The shown spline segments are part of a spline patch $\Omega^{(\ell)}$, where the blue edges have to be a part of the boundary $\partial\Omega$, and the green edges can be a part of the boundary $\partial\Omega$.

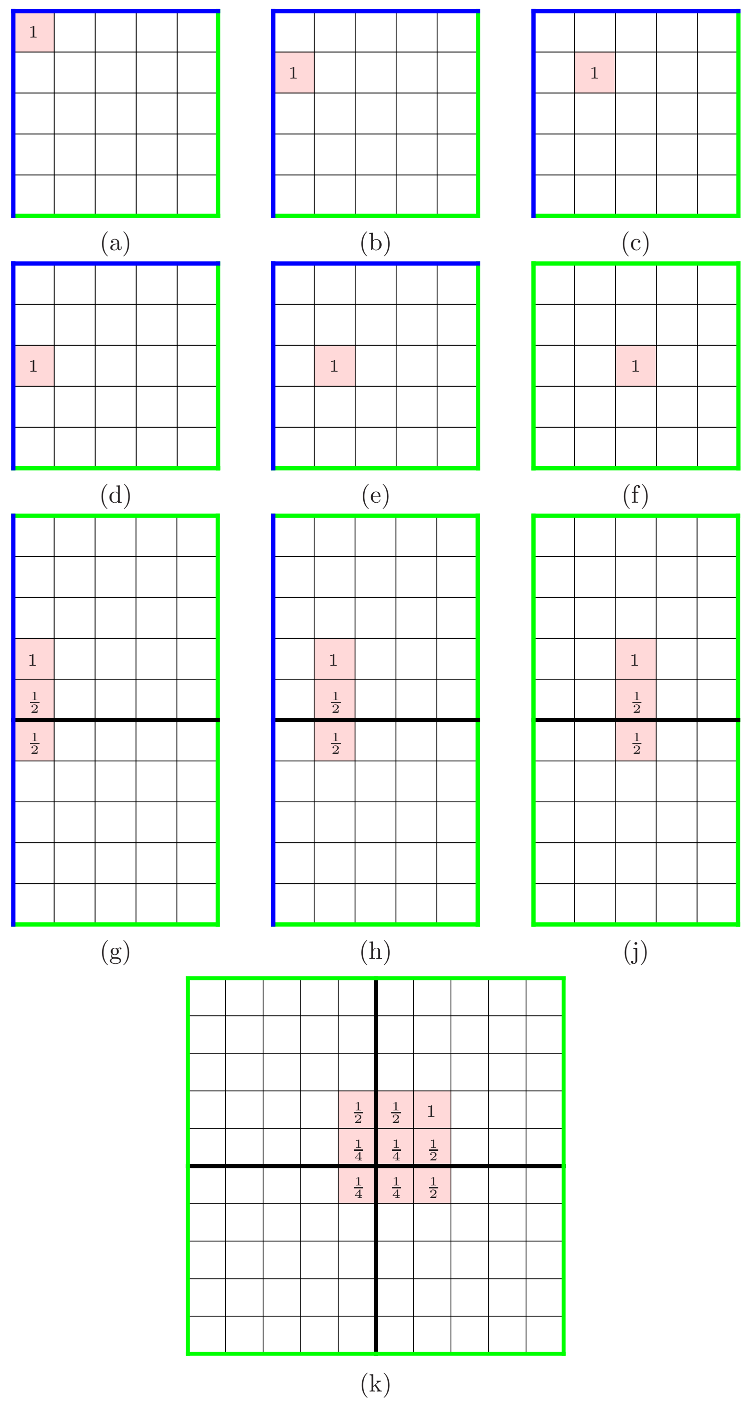

Figure 3: All possible supports $\mathrm{supp}_{\mathrm{BB}}(w)$ (red squares) of the patch basis functions w for $d = 4$ with the corresponding values of the Bézier coefficients $a_{\boldsymbol{i}}^{(\ell)}$ up to symmetries. The shown spline segments are part of a spline patch $\Omega^{(\ell)}$, where the blue edges have to be a part of the boundary $\partial\Omega$, and the green edges can be a part of the boundary $\partial\Omega$.

the patch basis functions, the Bézier coefficients $a_{\boldsymbol{i}}^{(\ell)}$ of the edge basis functions depend on the geometry mappings. The number of these functions was investigated in [10].

Lemma 1 ([10], Lemma 3 and Theorem 4)**.** *The number of linearly independent edge basis functions is equal to*

$$(2d+1)+(2d-4)k.$$

For $d = 4$, a possible choice of these $9+4k$ edge basis functions w was presented in [10], where the functions are categorized into 4 different types (A, B, L, U) with several subtypes. The classification is based on the size and location of their supports $\mathrm{supp}_{\mathrm{BB}}(w)$, see [10, Subsection 3.3 and Appendix]. The functions of type L and U are defined on the lower and upper boundary of the common interface, respectively, and the functions of type A and B are defined on inner parts of the common interface. The graphs of the different types of functions are visualized in [10, Fig. 6]. Since the functions of type L and U coincide with respect to swapping the lower boundary with the upper boundary of the two-patch domain, and vice versa, it sufficies to consider the functions of type L for the lower and upper boundary of the common interface. Fig. 5 shows the supports $\mathrm{supp}_{\mathrm{BB}}(w)$ of the functions w of type A, B and L for $d = 4$.

A similar choice of the $7+2k$ edge basis functions w for $d = 3$ is possible, too, where the functions are classified again with respect to their supports $\mathrm{supp}_{\mathrm{BB}}(w)$, see Fig. 4. In contrast to $d = 4$, the resulting functions of type A, B and L have slightly increased supports, but are located again on the boundary of the common interface for type L, and on inner parts of the common interface for type A and B. For both degrees, we present in Appendix A.1 more details about these different types of basis functions, including explicit formulas for their Bézier coefficients.

The following lemma guarantees that the basis functions of type A, B and L are a suitable choice of the $(2d+1)+(2d-4)k$ edge basis functions.

Lemma 2. *The* $(2d-9)+(2d-4)k$ *basis functions of type A and B for the inner part of the edge and the* 10 *basis functions of type L for the two boundaries of the edge (see Appendix A.1) are linearly independent.*

Proof. By using symbolic computation, it can be shown that the Bézier coefficient vector of each function is a solution of the homogeneous linear system (2). The linear independence of the functions can be proven by analyzing their Bézier coefficient vectors. □

The patch basis functions and the basis functions of type A, B and L form a basis of V.

Theorem 3 ([10], Theorem 6 for $d = 4$)**.** *The* $(2d-9)+(2d-4)k$ *basis functions of type A and B for the inner part of the edge and the* 10 *basis functions of type L for the two boundaries of the edge (see Appendix A.1), combined with the patch basis functions defined in* (3) *form a basis of the space of* C^1*-smooth geometrically continuous isogeometric functions.*

Proof. The number of the patch basis functions plus the number of the edge basis functions is equal to the dimension, and all the functions are linearly independent, compare [10, Theorem 4]. □

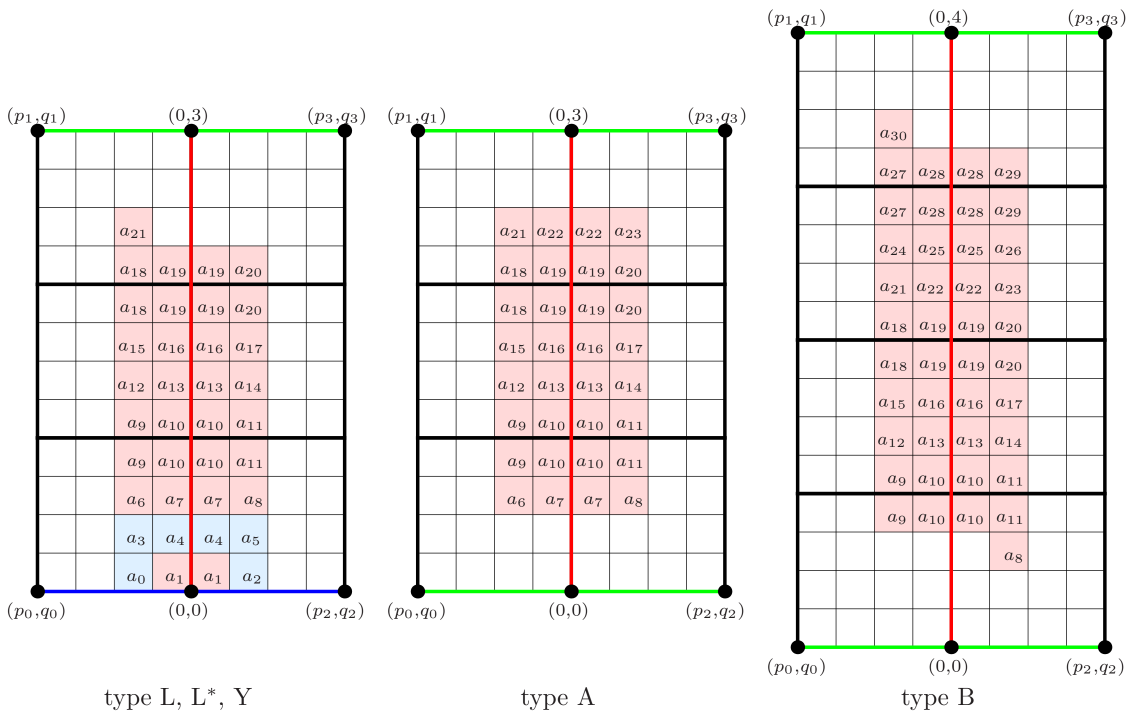

Figure 4: The maximal possible support in Bézier coefficient space $\mathrm{supp}_{\mathrm{BB}}(w)$ (red and blue squares) of the edge basis functions w of type A, B, L, L* and Y for $d = 3$. The shown spline segments are part of a two-patch domain $\Omega = \Omega^{(1)} \cup \Omega^{(2)}$. The red edges are part of the common interface of $\Omega^{(1)}$ and $\Omega^{(2)}$, the blue edges have to be a part of the boundary $\partial\Omega$, and the green edges can be a part of the boundary $\partial\Omega$. (See Appendix A for explicit formulas for the values a_i of the corresponding Bézier coefficients with respect to the given local geometry.)

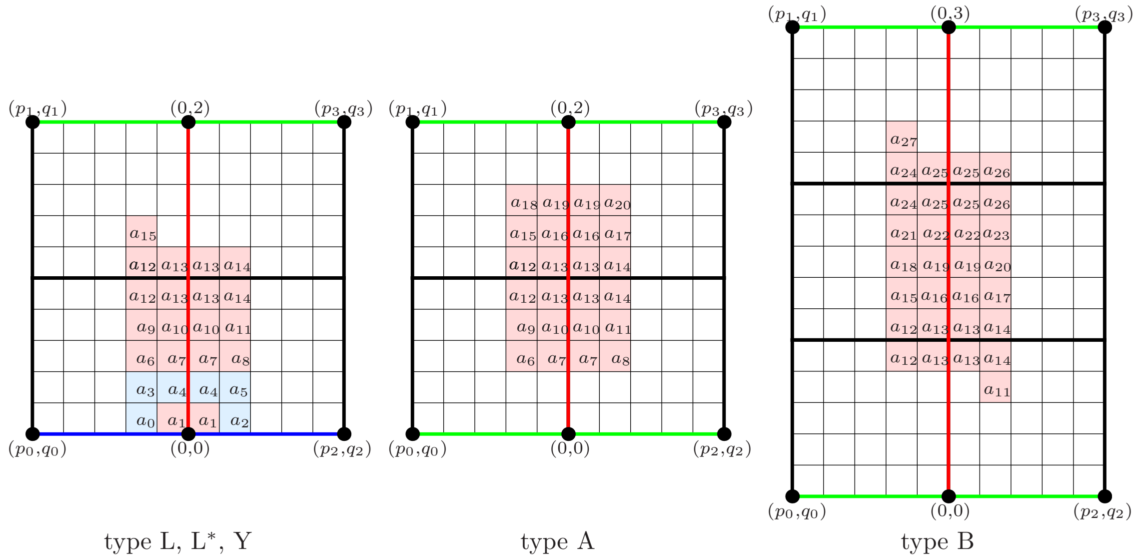

Figure 5: The maximal possible support in Bézier coefficient space $\mathrm{supp}_{\mathrm{BB}}(w)$ (red and blue squares) of the edge basis functions w of type A, B, L, L* and Y for $d = 4$. The shown spline segments are part of a two-patch domain $\Omega = \Omega^{(1)} \cup \Omega^{(2)}$. The red edges are part of the common interface of $\Omega^{(1)}$ and $\Omega^{(2)}$, the blue edges have to be a part of the boundary $\partial\Omega$, and the green edges can be a part of the boundary $\partial\Omega$. (See Appendix A for explicit formulas for the values a_i of the corresponding Bézier coefficients with respect to the given local geometry.)

Instead of the 5 basis functions of type L on the two boundaries of the common interface, we construct 5 different edge basis functions on these boundaries as follows. We select the 5 values a_0, a_2, a_3, a_4 and a_5 of the corresponding Bézier coefficients in such a way that one of them possesses the value one and the remaining values are zero, see Fig 4-Fig. 6. We refer to the resulting 5 basis functions as functions of type L*. For $d = 4$, the 5 different functions of type L* are visualized in Fig 7. In contrast to the functions of type L, these function of type L* are not well-defined if Assumption V is not fulfilled for the corresponding vertex of the common interface. The functions of type L* can be obtained by linearly combining the functions of type L, see Appendix A.2. We thus obtain:

Lemma 4. *Let $\boldsymbol{v}_0$ be one of the two vertices of the common interface of the two-patch domain Ω. If Assumption V is satisfied for the vertex $\boldsymbol{v}_0$, then the basis functions of type L* in the vicinity of $\boldsymbol{v}_0$ span the same space as the corresponding basis functions of type L.*

Proof. If Assumption V is satisfied for the common vertex $\boldsymbol{v}_0$, then all factors of the in Appendix A.2 presented linear combinations for the functions of type L* are well-defined. Since the basis functions of type L* are linearly independent due to their canonical construction, the corresponding basis functions of type L* span the same space as the corresponding basis functions of type L. □

Remark 5. Assumption IV is only needed to ensure that the functions of type A,B and L are linearly independent, which would be otherwise violated by the fact that $\mathrm{L}_1 = \mathrm{L}_2$. When using the functions of type L* instead of the functions of type L, the linear independence is still guaranteed in the case that Assumption IV is not fulfilled, but Assumption V is satisfied.

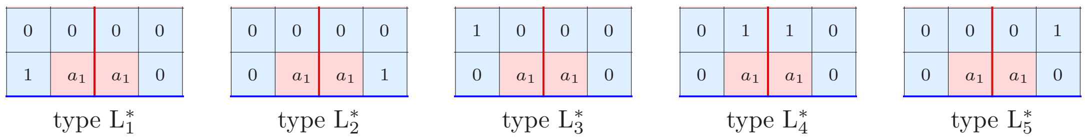

Figure 6: The 5 function of type L* are obtained by choosing the values a_i of the corresponding Bézier coefficients in the blue squares in Fig. 4 and 5 in the canonical way as shown. The value a_1 is equal to zero for the functions of type L$_3^*$ and L$_5^*$ and unequal to zero for the functions of type L$_1^*$, L$_2^*$ and L$_4^*$

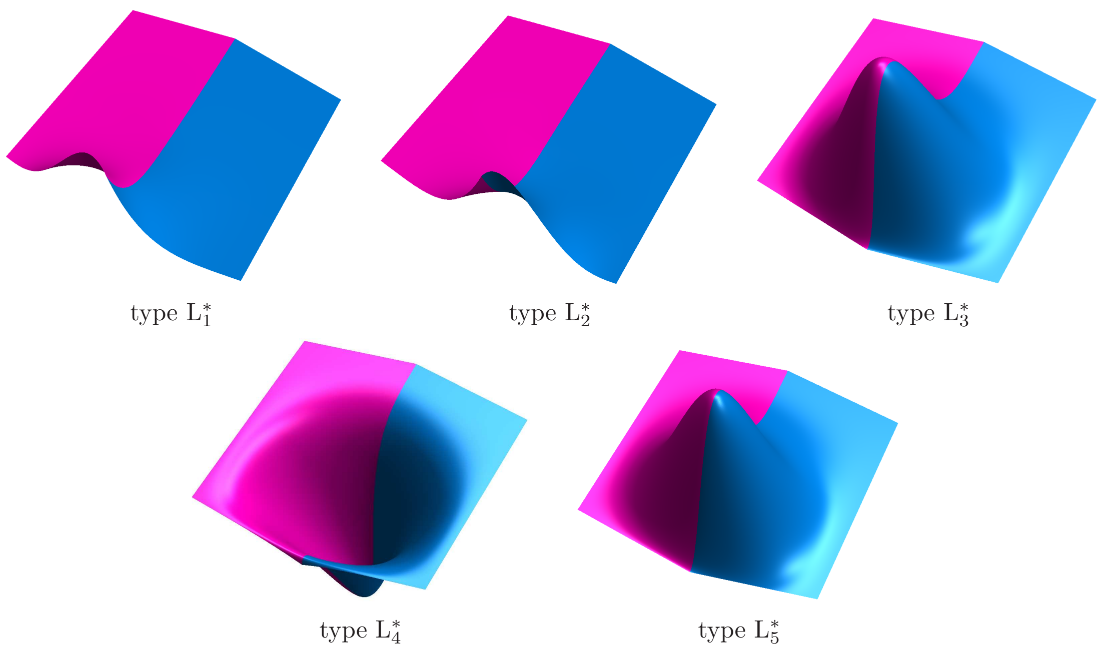

Figure 7: All different edge basis functions of type L* for $d = 4$. The formulas for the values of their corresponding Bézier coefficients are presented via linear combinations of the edge basis functions of type L in Appendix A.2.

4. C^1-smooth functions on bilinear multi-patch geometries

We present the construction of a basis of the space V of C^1-smooth geometrically continuous isogeometric functions on bilinearly parameterized multi-patch domains Ω. The obtained basis functions will be based on the different basis functions of two-patch domains from the previous section. Some of the functions coincide with a patch basis function or with a edge basis function of type A, B or L, and some of the functions are built from edge basis functions of type L*. In the following, we only consider multi-patch domains Ω that satisfy Assumptions I-V.

4.1. Basis functions from the two-patch case

For each two-patch domain $\Omega^{(\ell\ell')}$, $\ell, \ell' \in \{1, \ldots, n\}$ with $\ell \neq \ell'$, we can extend the resulting basis functions w from the previous section to the whole multi-patch domain Ω by setting all Bézier coefficients $a_{\boldsymbol{i}}^{(p)}$ of the additional patches $\Omega^{(p)}$, $p \in \{1, \ldots, n\}$ with $p \neq \ell$ and $p \neq \ell'$, to zero. For this, we define the following operator Q:

Definition 6. Let w be an isogeometric function on a two-patch domain $\Omega^{(\ell\ell')}$, $\ell, \ell' \in \{1, \ldots, n\}$ with $\ell \neq \ell'$, possessing a Bézier coefficient vector

$$\boldsymbol{a} = (a_{\boldsymbol{i}}^{(p)})_{p \in \{\ell, \ell'\}, \boldsymbol{i} \in \tilde{I}}.$$

The operator Q generates the Bézier coefficient vector $Q\boldsymbol{a} = \bar{\boldsymbol{a}}$ with

$$\bar{\boldsymbol{a}} = \left(a_{\boldsymbol{i}}^{(p)}\right)_{(p,\boldsymbol{i}) \in I}$$

and

$$\bar{\boldsymbol{a}}_{\boldsymbol{i}}^{(p)} = \begin{cases} a_{\boldsymbol{i}}^{(p)} & \text{if } p \in \{\ell, \ell'\} \\ 0 & \text{else} \end{cases}$$

for $(p, \boldsymbol{i}) \in I$.

In the following, we define $w_{\bar{\boldsymbol{a}}}$ to be the isogeometric function on Ω, that is determined by the Bézier coefficient vector $\bar{\boldsymbol{a}} = (\bar{a}_{\boldsymbol{i}}^{\ell})_{(\ell,\boldsymbol{i}) \in I}$. Let us consider the C^1-smooth geometrically continuous isogeometric basis functions w for two-patch domains from the previous section, which possess the Bézier coefficient vectors $\boldsymbol{a}$ for the corresponding two-patch domains. Clearly, $w_{Q\boldsymbol{a}} \in L^2(\Omega)$, but not all functions $w_{Q\boldsymbol{a}}$ are C^1-smooth on the whole multi-patch domain Ω.

Lemma 7. *For each two-patch domain $\Omega^{(\ell\ell')}$, $\ell, \ell' \in \{1, \ldots, n\}$ with $\ell \neq \ell'$, we compute the Bézier coefficient vectors $\boldsymbol{a}$ of all patch basis functions and edge basis functions of type A, B, L and L^*. Then an extended function $w_{Q\boldsymbol{a}}$ is C^1-smooth on Ω if and only if the initial isogeometric function on the two-patch domain $\Omega^{(\ell\ell')}$, i.e. $w_{Q\boldsymbol{a}}|_{\Omega^{(\ell\ell')}}$, is*

- *one of the patch basis functions (f), (j) and (k) from Fig 2 and 3, or*
- *one of the patch basis functions (a)-(e) and (g)-(h) from Fig 2 and 3, for which all boundary edges of $\partial\Omega^{(\ell\ell')}$ still are the boundary edges of $\partial\Omega$, or*
- *an edge basis function of type A or B, or*
- *an edge basis functions of type L or L^* with a support in the vicinity of a boundary vertex of valence $m = 3$.*

Proof. This can be easily verified by analyzing the smoothness of the resulting functions on Ω. □

We notice that we do not get any C^1-smooth function on Ω, possessing non-zero Bézier coefficients $a_{\boldsymbol{i}}^{(\ell)}$ in the vicinity of an inner vertex or a boundary vertex of valence $m \geq 4$. The following subsection explains the construction of such C^1-smooth geometrically continuous isogeometric basis functions on Ω.

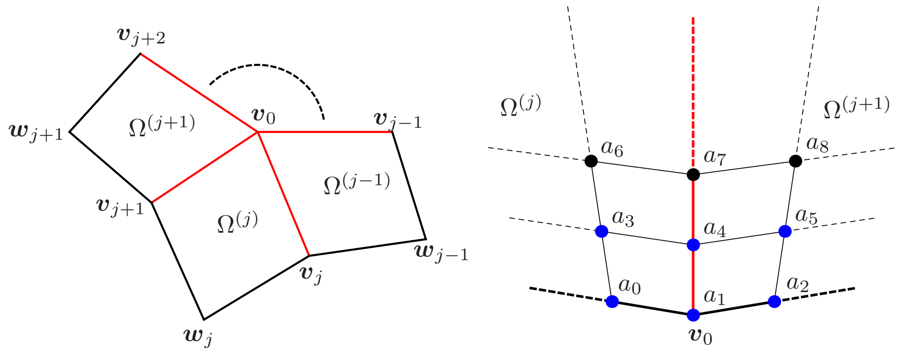

Figure 8: Left: An inner vertex $\boldsymbol{v}_0$ of valence $m \geq 3$ with the m neighboring patches $\Omega^{(j)}$ in clockwise order around the vertex $\boldsymbol{v}_0$. Right: The 6 values a_i, $i \in \{0, \ldots, 5\}$, of the Bézier coefficients (blue vertices) of the two-patch domain $\Omega^{(j((j+1) \bmod m))}$, which correspond to the inner vertex $\boldsymbol{v}_0$ or to the Bézier control points in the one-ring neighboorhood of $\boldsymbol{v}_0$. (Here, the Bézier coefficients along the common interface (red edge) are drawn only once for both patches, since their values are equal.)

4.2. Vertex basis functions

The edge basis functions of type L* will be used to generate C^1-smooth geometrically continuous isogeometric basis functions with non-zero Bézier coefficients $a_{\boldsymbol{i}}^{(\ell)}$ in the vicinity of the inner vertices and boundary vertices of valence $m \geq 4$. We first describe the construction of these functions in the case of inner vertices and will later slightly adapt this construction to the boundary vertices. For both cases, we will call the resulting C^1-smooth functions *vertex basis functions*.

Let us consider an inner vertex $\boldsymbol{v}_0$ of the multi-patch domain Ω of valence $m \geq 3$, and assume without loss of generality that the m neighboring patches $\Omega^{(j)}$, $j \in \{1, \ldots, m\}$, are given in a clockwise order around the vertex $\boldsymbol{v}_0$, see Fig. 8 (left). For each two patch domain $\Omega^{(j((j+1) \bmod m))}$, $j \in \{1, \ldots, m\}$, we generate 5 new edge basis functions denoted by type Y_1-Y_5. Their values a_i, $i \in \{0, \ldots, 5\}$, of the possibly non-zero Bézier coefficients that correspond to the inner vertex $\boldsymbol{v}_0$ or to the Bézier control points in the one-ring neighborhood of $\boldsymbol{v}_0$, see Fig. 4, 5 and 8(right), are determined as follows:

- Y_1: $a_0 = 1$, $a_1 = 1$, $a_2 = 1$, $a_3 = 0$, $a_4 = 1$, $a_5 = 0$.
- Y_2: $a_1 = 0$, $a_3 = 0$, $a_5 = 0$. The remaining values a_0, a_2 and a_4 are obtained by satisfying the conditions $w(\boldsymbol{v}_0) = 0$ and $\nabla w(\boldsymbol{v}_0) = (1, 0)^T$ with respect to the global coordinates for the corresponding isogeometric function w .
- Y_3: $a_1 = 0$, $a_3 = 0$, $a_5 = 0$. The remaining values a_0, a_2 and a_4 are obtained by satisfying the conditions $w(\boldsymbol{v}_0) = 0$ and $\nabla w(\boldsymbol{v}_0) = (0, 1)^T$ with respect to the global coordinates for the corresponding isogeometric function w.
- Y_4: $a_0 = 0$, $a_1 = 0$, $a_2 = 0$, $a_3 = 1$, $a_4 = 0$, $a_5 = 0$.
- Y_5: $a_0 = 0$, $a_1 = 0$, $a_2 = 0$, $a_3 = 0$, $a_4 = 0$, $a_5 = 1$.

The resulting 5 edge basis functions of type Y can be represented as a linear combination of the 5 edge basis functions of type L*, see Appendix A.3.

Lemma 8. *Let $\Omega^{(j((j+1) \bmod m))}$, $j \in \{1, \dots, m\}$, be a two-patch domain with the common vertex $\boldsymbol{v}_0$. The edge basis functions of type Y span the same space as the edge basis functions of type L*.*

Proof. It suffices to show that the basis functions of type Y are linearly independent which is trivially satisfied due to the selection of the values a_i, $i \in \{0, \dots, 5\}$, of the corresponding Bézier coefficients. $\square$

Let us denote the Bézier coefficient vectors of the isogeometric functions of type Y$_i$ by $\boldsymbol{a}^{(i,j)}$, $i \in \{1, \dots, 5\}$, $j \in \{1, \dots, m\}$. Clearly, the functions $w_{Q\boldsymbol{a}^{(i,j)}}$ are C^1-smooth within all single patches $\Omega^{(\ell)}$, $\ell \in \{1, \dots, n\}$, but cannot be C^1-smooth at some common interfaces of neighboring patches of Ω. We investigate these interfaces but first we define:

Definition 9. Let w be an isogeometric function on Ω with a Bézier coefficient vector $\boldsymbol{a}$. We define $D_{\boldsymbol{a}}$ to be the collections of those common interfaces of neighboring patches of Ω, where w is not C^1-smooth, i.e.

$$D_{\boldsymbol{a}} = \{\text{all patch interfaces } \boldsymbol{e} \text{ of } \Omega \mid w \text{ is not } C^1\text{-smooth at } \boldsymbol{e}\}.$$

Lemma 10. *Let $j \in \{1, \dots, m\}$. The sets $D_{Q\boldsymbol{a}^{(i,j)}}$, $i \in \{1, \dots, 5\}$, are given by*

$$D_{Q\boldsymbol{a}^{(i,j)}} = \{\boldsymbol{e}^{(j(j-1) \bmod m)}, \boldsymbol{e}^{((j+1) \bmod m(j+2) \bmod m)}\} \text{ for } i \in \{1, 2, 4\},$$

and by

$$D_{Q\boldsymbol{a}^{(3,j)}} = \{\boldsymbol{e}^{(j(j-1) \bmod m)}\},\ D_{Q\boldsymbol{a}^{(5,j)}} = \{\boldsymbol{e}^{((j+1) \bmod m(j+2) \bmod m)}\}.$$

Proof. This can be easily checked by analyzing the different functions $w_{Q\boldsymbol{a}^{(i,j)}}$ for $i \in \{1, \dots, 5\}$ with respect to C^1-smoothness across all common interfaces. $\square$

We will generate the vertex basis functions for the inner vertex $\boldsymbol{v}_0$, by assembling them from different functions $w_{Q\boldsymbol{a}^{(i,j)}}$. For this, we first define the operator, which will be used later to construct the Bézier coefficients of the vertex basis functions.

Definition 11. Let

$$\widetilde{\boldsymbol{a}} = \left(\tilde{a}_{\boldsymbol{i}}^{(\ell)}\right)_{(\ell,\boldsymbol{i}) \in I} \text{ and } \widehat{\boldsymbol{a}} = \left(\hat{a}_{\boldsymbol{i}}^{(\ell)}\right)_{(\ell,\boldsymbol{i}) \in I}$$

be the Bézier coefficient vectors of two isogeometric functions on Ω. The operator $\oplus$ generates the Bézier coefficient vector

$$\widetilde{\boldsymbol{a}} \oplus \widehat{\boldsymbol{a}} = \boldsymbol{a}$$

with

$$\boldsymbol{a} = \left(a_{\boldsymbol{i}}^{(\ell)}\right)_{(\ell,\boldsymbol{i}) \in I}$$

and

$$a_{\boldsymbol{i}}^{(\ell)} = \begin{cases} \tilde{a}_{\boldsymbol{i}}^{(\ell)} & \text{if } \hat{a}_{\boldsymbol{i}}^{(\ell)} = 0 \\ \hat{a}_{\boldsymbol{i}}^{(\ell)} & \text{if } \tilde{a}_{\boldsymbol{i}}^{(\ell)} = 0 \\ \tilde{a}_{\boldsymbol{i}}^{(\ell)} & \text{if } \tilde{a}_{\boldsymbol{i}}^{(\ell)} = \hat{a}_{\boldsymbol{i}}^{(\ell)} \\ \text{undefined} & \text{else} \end{cases}$$

for $(\ell, \boldsymbol{i}) \in I$.

Note that, if all coefficients $a_{\boldsymbol{i}}^{(\ell)}$ are well-defined, then the Bézier coefficient vector $\boldsymbol{a}$ defines an isogeometric function w on Ω. In addition, the operator $\oplus$ is commutative and associative. We will need later the following lemma.

Lemma 12. *Let $\widetilde{\boldsymbol{a}}$ and $\widehat{\boldsymbol{a}}$ be the Bézier coefficient vectors of the two isogeometric functions $\widetilde{w}$ and $\widehat{w}$, respectively, both defined on Ω, and assume that all Bézier coefficients $a_{\boldsymbol{i}}^{(\ell)}$ of $\boldsymbol{a} = \widetilde{\boldsymbol{a}} \oplus \widehat{\boldsymbol{a}}$ are well-defined. If $\boldsymbol{e} \in D_{\widetilde{\boldsymbol{a}}}$, $\boldsymbol{e} \notin D_{\widehat{\boldsymbol{a}}}$ and $\mathrm{supp}_{\mathrm{BB}}(\widetilde{w}) \cap I_{\boldsymbol{e}} \subset \mathrm{supp}_{\mathrm{BB}}(\widehat{w}) \cap I_{\boldsymbol{e}}$, then*

$$\boldsymbol{e} \notin D_{\boldsymbol{a}}.$$

Proof. For $(\ell, \boldsymbol{i}) \in I_{\boldsymbol{e}}$, the Bézier coefficients $a_{\boldsymbol{i}}^{(\ell)}$ coincide with the Bézier coefficients $\hat{a}_{\boldsymbol{i}}^{(\ell)}$, and therefore, the function $w_{\boldsymbol{a}}$ is also C^1-smooth at $\boldsymbol{e}$. $\square$

We generate now $3+m$ vertex basis functions for the inner vertex $\boldsymbol{v}_0$, where the Bézier coefficient vectors $\boldsymbol{a}$ of 3 functions are defined by

$$\boldsymbol{a} = \bigoplus_{j=1}^{m} Q\boldsymbol{a}^{(i,j)} \tag{4}$$

for $i \in \{1, \ldots, 3\}$, and the Bézier coefficient vectors $\boldsymbol{a}$ of m further functions are defined by

$$\boldsymbol{a} = Q\boldsymbol{a}^{(j,5)} \oplus Q\boldsymbol{a}^{((j+1) \bmod m, 4)} \tag{5}$$

for $j \in \{1, \ldots, m\}$. The resulting $m+3$ vertex basis functions are C^1-smooth on Ω.

Lemma 13. *All single Bézier coefficients $a_{\boldsymbol{i}}^{(\ell)}$ of the Bézier coefficient vectors $\boldsymbol{a}$ in* (4) *and* (5) *are well defined and the resulting vertex basis functions $w_{\boldsymbol{a}}$ are C^1-smooth on Ω.*

Proof. We first show that all resulting Bézier coefficients $a_{\boldsymbol{i}}^{(\ell)}$ of a vertex basis function are well-defined. We observe that the intersection of the supports $\mathrm{supp}_{\mathrm{BB}}(w)$ of any two different involved and to the multi-patch domain Ω extended functions w of type Y, can only contain Bézier coefficients that correspond to the vertex $\boldsymbol{v}_0$ and to the neighboring Bézier control points. Consequently, each resulting Bézier coefficient $a_{\boldsymbol{i}}^{(\ell)}$ of a vertex basis function that do not correspond to the vertex $\boldsymbol{v}_0$ or to a neighboring Bézier control point is trivially well-defined.

It remains to be shown that the remaining $4m$ Bézier coefficients $a_{\boldsymbol{i}}^{(\ell)}$ of a vertex basis function are well-defined, too. This is guaranteed by the choice of the values of the corresponding Bézier coefficients of the involved and to the multi-patch domain Ω extended functions of type Y. If a Bézier coefficient $a_{\boldsymbol{i}}^{(\ell)}$ of a vertex basis functions is contained in the intersection of the supports $\mathrm{supp}_{\mathrm{BB}}(w)$ of any two different involved and extended functions w of type Y, then the value of this Bézier coefficient is equal for both extended functions of type Y.

To show that a vertex basis functions w with the Bézier coefficient vector $\boldsymbol{a}$ is C^1-smooth on Ω, we subsequently apply Lemma 12 and obtain $D_{\boldsymbol{a}} = \emptyset$, which concludes the proof. $\square$

We will also call the first three vertex basis functions *proper vertex functions* and the remaining m vertex basis functions *twist functions*. An example of these 8 basis functions for an inner vertex $\boldsymbol{v}_0$ of valence 5 is visualized in Fig. 9.

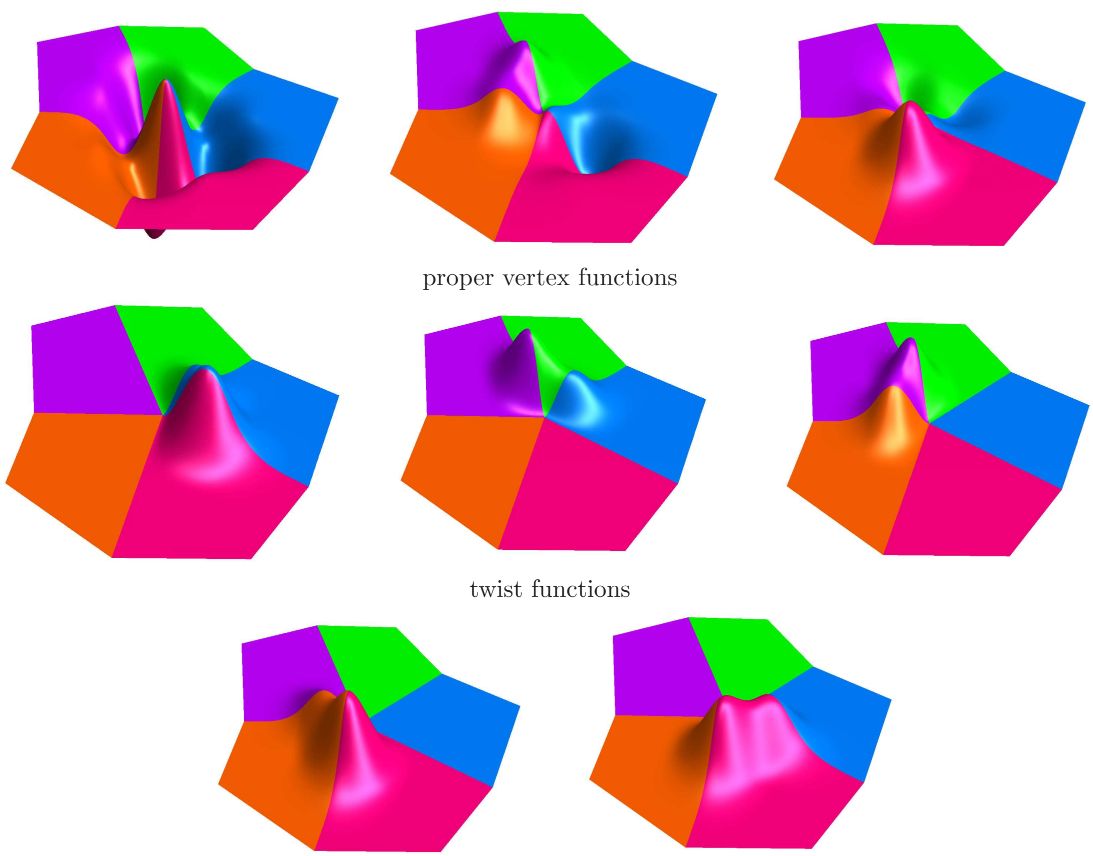

proper vertex functions

twist functions

twist functions

Figure 9: An example of all different vertex basis functions (i.e. 3 proper vertex functions and 5 twist functions) of an inner vertex of valence 5 for $d = 4$.

Slightly adapted, we can construct the vertex basis functions for a boundary vertex of valence $m \geq 4$. Let us consider such a boundary vertex $\boldsymbol{v}_0$ of the multi-patch domain Ω, and assume without loss of generality that the $m-1$ neighboring patches $\Omega^{(j)}$, $j \in \{1, \ldots, m-1\}$, are given in a clockwise order around the vertex $\boldsymbol{v}_0$ as visualized in Fig. 10. Again, we

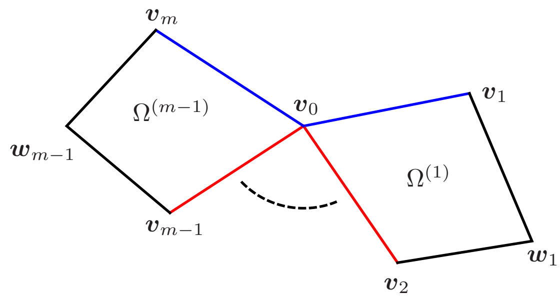

Figure 10: A boundary vertex $\boldsymbol{v}_0$ of valence $m \geq 4$ with the $m-1$ neighboring patches $\Omega^{(\ell)}$, $\ell \in \{1, \ldots, m-1\}$, in clockwise order around the vertex $\boldsymbol{v}_0$. The red edges are the common edges between two neighboring patches, and the blue edges are boundary edges of the multi-patch domain Ω.

compute first the functions of type Y for all two-patch domains $\Omega^{(j(j+1))}$, $j \in \{1, \ldots, m-2\}$, and denote the resulting Bézier coefficient vector of the function of type Y_i for the two-patch domains $\Omega^{(j(j+1))}$ by $\boldsymbol{a}^{(i,j)}$. We construct now $3 + (m-1)$ vertex basis functions for the boundary vertex $\boldsymbol{v}_0$, where the Bézier coefficient vectors $\boldsymbol{a}$ of 3 functions are defined by

$$\boldsymbol{a} = \bigoplus_{j=1}^{m-1} Q\boldsymbol{a}^{(i,j)} \tag{6}$$

for $i \in \{1, \ldots, 3\}$, the Bézier coefficient vectors $\boldsymbol{a}$ of $m-3$ functions are defined by

$$\boldsymbol{a} = Q\boldsymbol{a}^{(j,5)} \oplus Q\boldsymbol{a}^{(j+1,4)} \tag{7}$$

for $j \in \{1, \ldots, m-3\}$, and the Bézier coefficient vectors $\boldsymbol{a}$ of 2 functions are only defined by

$$\boldsymbol{a} = Q\boldsymbol{a}^{(1,4)} \text{ and } \boldsymbol{a} = Q\boldsymbol{a}^{(m-1,5)}. \tag{8}$$

Lemma 14. *All single Bézier coefficients $a_{\boldsymbol{i}}^{(\ell)}$ of the Bézier coefficient vectors $\boldsymbol{a}$ in* (6), (7) *and* (8) *are well defined and the resulting isogeometric functions $w_{\boldsymbol{a}}$ are C^1-smooth on Ω.*

Proof. Similar to the proof of Lemma 13, one can show that all single Bézier coefficients $a_{\boldsymbol{i}}^{(\ell)}$ of the resulting Bézier coefficient vectors $\boldsymbol{a}$ are well defined and that all functions are C^1-smooth on Ω. □

We will call again the first three vertex basis functions *proper vertex functions* and the remaining $m-1$ vertex basis functions *twist functions*.

4.3. Basis of the space

In the previous two subsections, we have explained the construction of different kinds of C^1-smooth geometrically continuous isogeometric functions on Ω. Let us now subdivide these functions into four sets $\mathcal{H}_i$ and investigate the cardinality ν_i of each resulting set $\mathcal{H}_i$, $i \in \{1, \ldots, 4\}$.

The set $\mathcal{H}^1$ consists of the patch basis functions extended to Ω, which are obtained for each spline control point of a geometry mapping $\boldsymbol{G}^{(\ell)}$, that does not belong to a common interface with a neighboring patch and to the neighboring column of spline control points. For each geometry mapping $\boldsymbol{G}^{(\ell)}$ the number of these functions depends on the number of common interfaces of the considered patch with its neighboring patches. In detail, this number $\nu_1^{(\ell)}$ is given by

$$\nu_1^{(\ell)} = \begin{cases} (d-1+k(d-1))(d+1+k(d-1)) \text{ for one interface,} \\ (d-1+k(d-1))^2 \text{ for two interfaces with common vertex,} \\ (d-3+k(d-1))(d+1+k(d-1)) \text{ for two interfaces without common vertex,} \\ (d-3+k(d-1))(d-1+k(d-1)) \text{ for three interfaces, and} \\ (d-3+k(d-1))^2 \text{ for four interfaces.} \end{cases}$$

Consequently, ν_1 is then obtained by summing up the resulting numbers of functions for the single patches, i.e.

$$\nu_1 = \sum_{i=1}^{n} \nu_1^{(i)}.$$

The set $\mathcal{H}^2$ contains for each common interface of two neighboring patches $\Omega^{(\ell)}$ and $\Omega^{(\ell')}$, $\ell, \ell' \in \{1, \ldots, n\}$ with $\ell \neq \ell'$, the $(2d-9) + (2d-4)k$ edge basis functions of type A and B extended to Ω. Therefore, ν_2 is equal to

$$\nu_2 = r_2((2d-9) + (2d-4)k),$$

where r_2 is the number of different such two-patch domains $\Omega^{(\ell\ell')}$.

The set $\mathcal{H}^3$ contains for each boundary vertex of valence $m = 3$ the 5 edge basis functions of type L extended to Ω. Consequently, ν_3 is equal to

$$\nu_3 = 5r_3,$$

where r_3 is the number of different vertices of valence $m = 3$.

The set $\mathcal{H}^4$ consists of the $3+m$ vertex basis functions for each inner vertex of valence m, and of the $3 + (m-1)$ vertex basis functions for each boundary vertex of valence $m \geq 4$. Therefore, ν_4 is given by

$$\nu_4 = \sum_{\boldsymbol{v}:\text{type I vertex (inner)}} (3 + m_{\boldsymbol{v}}) + \sum_{\boldsymbol{v}:\text{type I vertex (boundary)}} (3 + m_{\boldsymbol{v}} - 1),$$

where $m_{\boldsymbol{v}}$ is the valence of the vertex $\boldsymbol{v}$.

The union of these sets, i.e. $\mathcal{H} = \cup_{i=1}^{4} \mathcal{H}^i$, is a basis of V.

Theorem 15. *The set $\mathcal{H}$ is a basis of the space V of C^1-smooth geometrically continuous isogeometric functions defined on Ω.*

PROOF. We will show that each function $w \in V$ can be uniquely represented as a linear combination of the functions of $\mathcal{H}$, i.e.

$$w(\boldsymbol{x}) = \sum_{i=1}^{4} \sum_{j=1}^{\nu_i} \lambda_j^i z_j^i(\boldsymbol{x}), \quad \boldsymbol{x} \in \Omega,$$

where z_j^i are the functions of the set $\mathcal{H}^i$ and λ_j^i are the corresponding coefficients.

Clearly, each function $w \in V$ possesses a unique Bézier representation. Let us consider two different types of sets of Bézier coefficients, denoted by $\mathcal{A}^{(\ell)}$ and $\mathcal{A}^{(\ell\ell')}$, where

$$\mathcal{A}^{(\ell)} = \{a_{\boldsymbol{i}}^{(\ell)} \mid (\ell, \boldsymbol{i}) \notin I_{\boldsymbol{e}^{(\ell\ell')}} \text{ for } \ell' \in \{1, \ldots, n\} \text{ with } \ell' \neq \ell\}$$

and

$$\mathcal{A}^{(\ell\ell')} = \{a_{\boldsymbol{i}}^{(\ell)} \mid (\ell, \boldsymbol{i}) \in I_{\boldsymbol{e}^{(\ell\ell')}}\} \cup \{a_{\boldsymbol{i}}^{(\ell')} \mid (\ell', \boldsymbol{i}) \in I_{\boldsymbol{e}^{(\ell\ell')}}\}.$$

Consequently, the union of all sets $\mathcal{A}^{(\ell)}$ and $\mathcal{A}^{(\ell\ell')}$ is an overlapping decomposition of the set $\mathcal{A}$ of all Bézier coefficients $a_{\boldsymbol{i}}^{(\ell)}$ of w. In the following, we consider only non-empty sets $\mathcal{A}^{(\ell)}$ and $\mathcal{A}^{(\ell\ell')}$.

For a set $\mathcal{F}$ of functions on Ω, we denote by $\mathcal{F}|_{\mathcal{A}^{(\ell)}}$ and $\mathcal{F}|_{\mathcal{A}^{(\ell\ell')}}$ the set of those non-zero functions, which are obtained by restricting the functions of $\mathcal{F}$ to the Bézier coefficients $a_{\boldsymbol{i}}^{(\ell)}$ from the set $\mathcal{A}^{(\ell)}$ and $\mathcal{A}^{(\ell\ell')}$, respectively. Our construction of the functions of $\mathcal{H}$ ensures that each set of function $\mathcal{H}|_{\mathcal{A}^{(\ell)}}$ and $\mathcal{H}|_{\mathcal{A}^{(\ell\ell')}}$ is a basis of $V|_{\mathcal{A}^{(\ell)}}$ and $V|_{\mathcal{A}^{(\ell\ell')}}$, respectively. In case of each set $\mathcal{A}^{(\ell)}$ the set of resulting functions consists of $\nu_1^{(\ell)}$ linearly independent patch basis functions, which span the space $V|_{\mathcal{A}^{(\ell)}}$, and in case of each set $\mathcal{A}^{(\ell\ell')}$ the set of resulting functions consists of $(2d+1)+(2d-4)k$ linearly independent edge basis functions, which span the space $V|_{\mathcal{A}^{(\ell\ell')}}$, compare Lemma 1, 2, 4 and 8. Therefore, a function $w \in V$ has a unique representation

$$w|_{\bar{\mathcal{A}}} = \sum_{i=1}^{4} \sum_{j=1}^{\nu_i} \lambda_j^i z_j^i|_{\bar{\mathcal{A}}} \tag{9}$$

for each set $\bar{\mathcal{A}}$ equal to a set $\mathcal{A}^{(\ell)}$ or $\mathcal{A}^{(\ell\ell')}$ (or more precisely, unique coefficients λ_j^i for the non-zero functions $z_j^i|_{\bar{\mathcal{A}}}$).

It remains to be shown that each coefficient λ_j^i has to be uniquely determined for all representations (9), where the corresponding function z_j^i is not the zero function. For the coefficients λ_j^i with $i \in \{1, 2, 3\}$, this is trivially satisfied, since each function $z_j^i|_{\bar{\mathcal{A}}}$, $i \in \{1, 2, 3\}$, is a non-zero function exactly for one set $\bar{\mathcal{A}}$ ($\mathcal{A}^{(\ell)}$ for $i = 1$ and $\mathcal{A}^{(\ell\ell')}$ for $i = 2, 3$). To show that the coefficients λ_j^4 are also uniquely determined, we use the fact that each function z_j^4 is generated in such a way that each Bézier coefficient $a_{\boldsymbol{i}}^{(\ell)}$ of z_j^4 is uniquely determined for all functions $z_4^i|_{\mathcal{A}^{(\ell\ell')}}$ with $a_{\boldsymbol{i}}^{(\ell)} \in \mathcal{A}^{(\ell\ell')}$, and that the functions $z_4^i|_{\mathcal{A}^{(\ell)}}$ are zero for all sets $\mathcal{A}^{(\ell)}$. $\square$

Proposition 16. *The dimension of the space V of C^1-smooth geometrically continuous isogeometric functions defined on Ω is equal to*

$$\dim V = \sum_{i=1}^{4} \nu_i.$$

PROOF. Since the cardinality of each set $\mathcal{H}^i$, $i \in \{1, \ldots, 4\}$, is given by the values ν_i, we directly obtain the dimension of V as the sum of these values. $\square$

Note, that a function $w \in V$ belong to the space $H^2(\Omega)$, since they are globally C^1-smooth and piecewise C^∞-smooth. This provides us a possibility to use them to solve amongst others the biharmonic equation over different multi-patch domains, which will be demonstrated on the basis of some examples in the following section.

5. Examples

We present several examples of using C^1-smooth geometrically continuous isogeometric functions on different multi-patch domains to perform L^2 approximation, to solve Poisson's equation or the biharmonic equation over these domains. For all three applications we consider the same model problems as described in [10, Section 4.1-4.3] for two-patch domains, and use the therein explained isogeometric approaches for solving the particular problems.

The first example numerically analyzes the approximation power of C^1-smooth geometrically continuous isogeometric functions on multi-patch domains.

Example 17. We consider three different multi-patch domains Ω, see Fig. 11 (first row), which consist of three, four and five quadrilateral patches $\Omega^{(\ell)}$, respectively. The corresponding geometry mappings $\boldsymbol{G}^{(\ell)}$ are bilinear parameterizations, which are represented as Bézier patches of degree (d, d) for $d \in \{3, 4\}$. For each multi-patch domain Ω the resulting geometry mappings $\boldsymbol{G}^{(\ell)}$ determine a space of C^1-smooth geometrically continuous isogeometric functions on Ω.

Analogous to the numerical results for two-patch domains in [10] we generate a sequence of nested spaces of C^1-smooth geometrically continuous isogeometric functions. By considering the B-splines patches $\boldsymbol{G}^{(\ell)} \in \mathcal{S}^d_{2^\lambda-1,d-1} \times \mathcal{S}^d_{2^\lambda-1,d-1}$, $\lambda \in \mathbb{N}_0$, we get a refined space of C^1-smooth geometrically continuous isogeometric functions on Ω. The resulting space will be denoted again by V_h, where $h = \mathcal{O}(2^{-\lambda})$ and λ is the level of refinement. We construct a basis for these spaces by using the method described in the previous sections. Thereby, we slightly modify the construction of some functions for low levels, i.e. for $\lambda = 0, 1$ for $d = 3$ and for $\lambda = 0$ for $d = 4$, since our general method does not work for these levels. More precisely, we construct for these levels a basis of the nullspace of H or of $\tilde{H}$ of the homogeneous system (1) or (2), respectively, in a different way.

By additionally requiring that the functions $w \in V_h$ have to satisfy the homogeneous boundary conditions

$$w_i(\boldsymbol{x}) = 0 \text{ on } \partial\Omega \tag{10}$$

and

$$w_i(\boldsymbol{x}) = \frac{\partial w_i}{\partial \boldsymbol{n}}(\boldsymbol{x}) = 0 \text{ on } \partial\Omega, \tag{11}$$

we can generate a sequence of nested spaces which can be used for solving Poisson's equation and the biharmonic equation, respectively. These spaces will be denoted again by $V_{0,0h}$ and $V_{1,0h}$, respectively. A basis of these spaces can be obtained from the corresponding basis of V_h by removing those boundary basis functions w which do not satisfy the appropriate boundary conditions. Note, that for $d = 3$ the coarsest level for the space $V_{1,0h}$ start with

$\lambda = 1$, since there do not exist C^1-smooth geometrically continuous isogeometric functions, which satisfy the boundary conditions (11) for $\lambda = 0$.

We use the resulting C^1-smooth geometrically continuous isogeometric functions to solve three different applications on the three multi-patch domains (i.e. three-, four- and five patch domain). First, we approximate for all three domains the function

$$z(x_1, x_2) = 2\cos(2x_1)\sin(2x_1),$$

shown in Fig. 11 (second row). Second, we numerically solve Poisson's equation over the three domains. The different right-hand side functions f of Poisson's equation (cf. [10, Eq. (16)]) are obtained by differentiating the functions

$$u(x_1, x_2) = \frac{1}{C}\prod_{i=1}^{2n} \boldsymbol{e}_i(x_1, x_2),$$

where C is some different constant for each domain and $\boldsymbol{e}_i$ are the lines defined by the boundary edges of the domains. Third, we numerically solve the biharmonic equations over the three domains, where the different right-hand side functions f of the biharmonic equation (cf. [10, Eq. (18)]) are obtained by differentiating the corresponding functions $\tilde{u} = u^2$. The functions u and $\tilde{u}$ satisfy the homogeneous boundary conditions (10) and (11), respectively, and are visualized in Fig. 11 (third row) and Fig. 11 (fourth row), respectively.

We present the resulting relative H^i-errors ($i = 0$ for L^2-approximation, $i = 0, 1$ for Poisson's equation and $i = 0, 1, 2$ for biharmonic equation) for the different level λ of refinement in Fig. 12. For all three applications the numerical results indicate an optimal convergence rate of $\mathcal{O}(h^{d+1-i})$ in the associated H^i-norms, $i = 0, 1, 2$.

The following example explores two possibilities from [10, Section 3.4] to deal with more general domains.

Example 18. As first example we consider a domain with hole consisting of four quadrilateral patches, see Fig. 13 (first row). We have relaxed the requirement of bilinear patches by modifying some control points, which do not affect the edge basis functions and vertex basis functions. This allows us to construct the shown computational domain with a curved boundary around the hole. Similar to Ex. 17, we solve Poisson's equation with the right-hand side function f obtained by differentiating the function

$$u(x_1, x_2) = \frac{1}{1000}(x_1 - 5)(x_1 + 5)(x_2 - 5)(x_2 + 5)({x_1}^2 + {x_2}^2 - \frac{9}{4}),$$

and with the non-homogeneous Dirichlet boundary conditions derived from this function u. Fig. 13 shows the exact solution u (second row) and the resulting relative H^i-errors, $i = 0, 1$ (third row) by using biquartic functions for solving Poisson's equation on a refined mesh.

The second computational domain, which is modeled after a car part, see Fig. 13 (first row), was constructed by following the second generalization from [10, Section 3.4]. First, we choose a bilinear reference geometry $\bar{\boldsymbol{G}}$ of the target geometry (i.e the desired car part), where the geometry mapping $\bar{\boldsymbol{G}}$ consists of five patches $\bar{\boldsymbol{G}}^{(\ell)} \in \mathcal{S}^4_{3,3} \times \mathcal{S}^4_{3,3}$. Second,

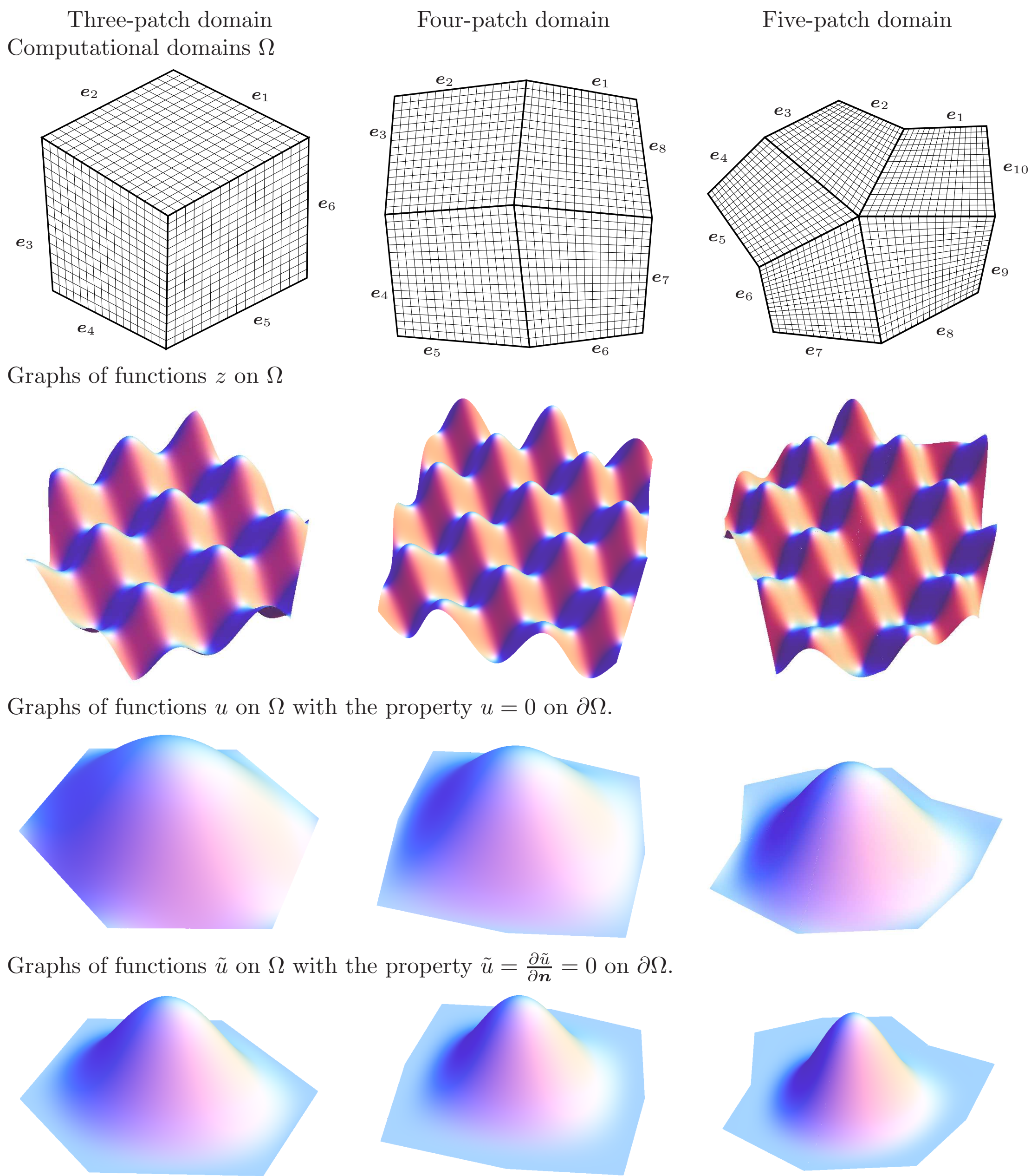

Figure 11: Three different multi-patch domains as computational domains (first row) with the exact solutions z for L^2-approximation (second row), the exact solutions u for solving Poisson's equation (third row) and the exact solutions $\tilde{u}$ for solving the biharmonic equations (fourth row).

we compute for this reference geometry a basis of the corresponding space $\bar{V}$ of C^1-smooth geometrically continuous isogeometric functions. Third, we fit the target geometry by using L^2-approximation for each coordinate function to achieve a geometry mapping $\boldsymbol{G} \in \bar{V} \times \bar{V}$, which describes the car part, and where the common interfaces do not resemble solely

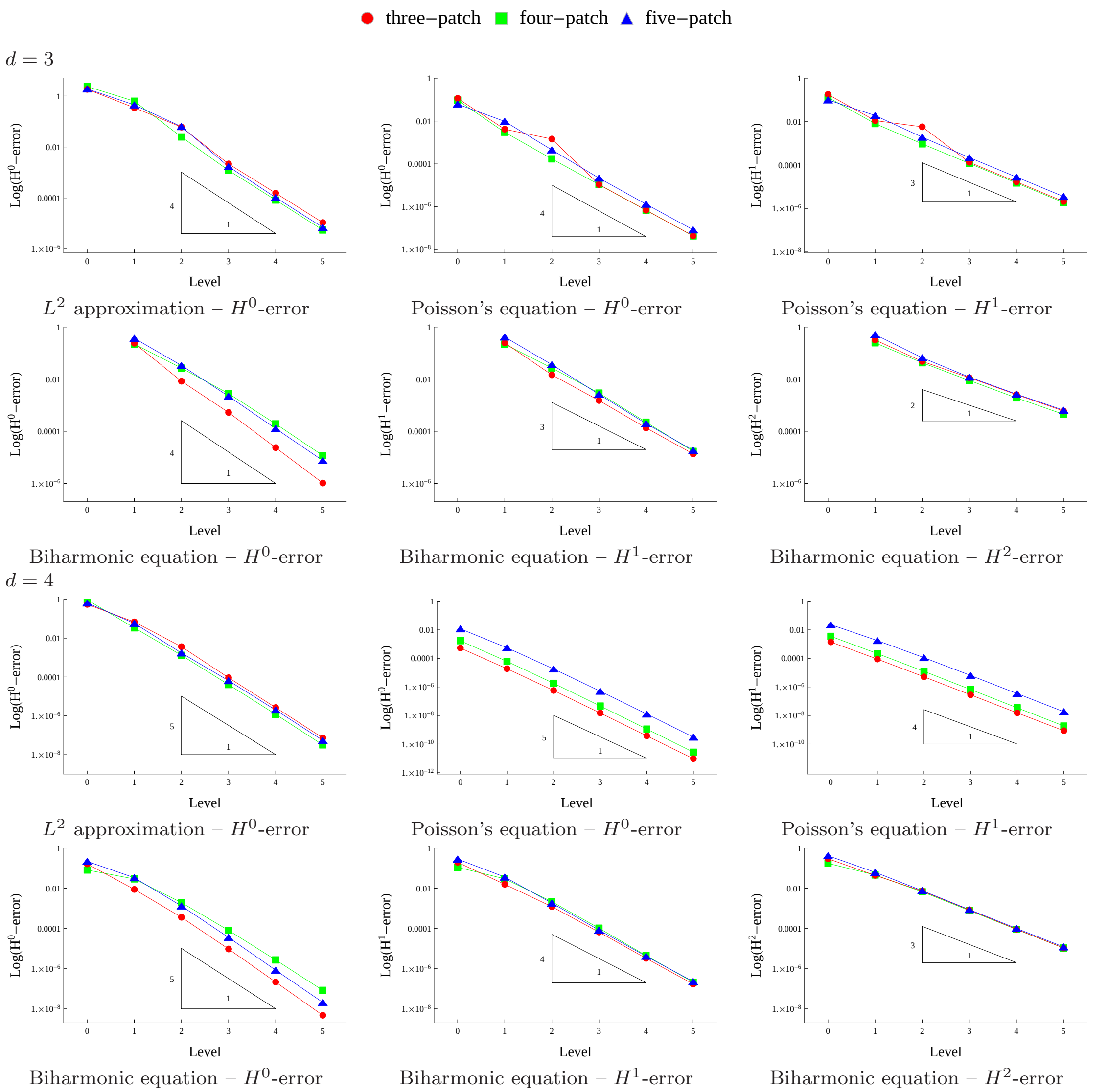

Figure 12: The relative H^i-errors by performing L^2 approximation ($i = 0$), solving Poisson's equation ($i = 0, 1$) and solving the biharmonic equation ($i = 0, 1, 2$) over the three different multi-patch domains given in Fig. 11. The estimated convergence rates (i.e. the dyadic logarithm of the ratio of two consecutive relative errors) are demonstrated with the help of the corresponding slope triangles.

straight lines. This construction of the computational domain ensures that the associated basis functions possess the same Bézier coefficients as the basis functions for the reference geometry. Similar to the domain with hole, we solve Poisson's equation with the right-hand side f obtained by the exact solution

$$u(x_1, x_2) = \frac{1}{5000}(4-x_2)(4+\frac{5x_1}{3}-x_2)(\frac{3}{2}-x_2)(x_1+5)(-\frac{7}{2}-x_2)({x_1}^2+(x_2+\frac{7}{2})^2-4)(x_1-5)$$

see Fig. 13(second row), and with the corresponding non-homogeneous Dirichlet boundary conditions. The resulting relative H^i-errors, $i = 0, 1$ by using biquartic functions for solving Poisson's equation over the fitted domain are visualized in Fig 13 (third row).

6. Conclusion

We constructed a basis of the space V of bicubic and biquartic C^1-smooth geometrically continuous isogeometric functions on bilinearly parameterized multi-patch domains $\Omega \subset \mathbb{R}^2$. The resulting basis functions are based on C^1-smooth functions from the two patch case (cf. [10]) and can be easily obtained by means of explicit formulas for the Bézier coefficients of their spline segments. We also presented numerical experiments of using the obtained bicubic and biquartic C^1-smooth isogeometric functions for different applications, which showed optimal rates of convergence.

The paper leaves several open issues for possible future research. One such topic consists in the theoretical investigation of the approximation power of the space of C^1-smooth geometrically continuous isogeometric functions defined on bilinear multi-patch domains. We expect them to possess the full aproximation power, since the space of these functions contains cubic and quartic polynomials on the domain.

Another challenging topic is the construction of geometrically continuous isogeometric functions of higher degree and/or smoothness. We have already demonstrated the potential of the geometrically continuous isogeometric functions by solving the biharmonic equation. The exploration of further possible applications, which require these functions of higher smoothness, is of interest, too. Finally, the extension of the framework to the three-dimensional case will be considered.

Appendix A. Edge basis functions

In [10], we specified for $d = 4$ simple explicit formulas for the Bézier coefficients of the edge basis functions [1] for bilinearly parameterized two-patch domains Ω. In this section, we recall these formulas in a slightly more compact way, and present similar ones for $d = 3$. Moreover, we add for both degrees two further possible choices of the Bézier coefficients of the edge basis functions on the boundaries of the common interface of the two-patch domain, which are obtained as linear combinations of the initial boundary functions.

[1] These functions were called in [10] basis function of the second kind.

Domain with hole | Car part

Computational domains

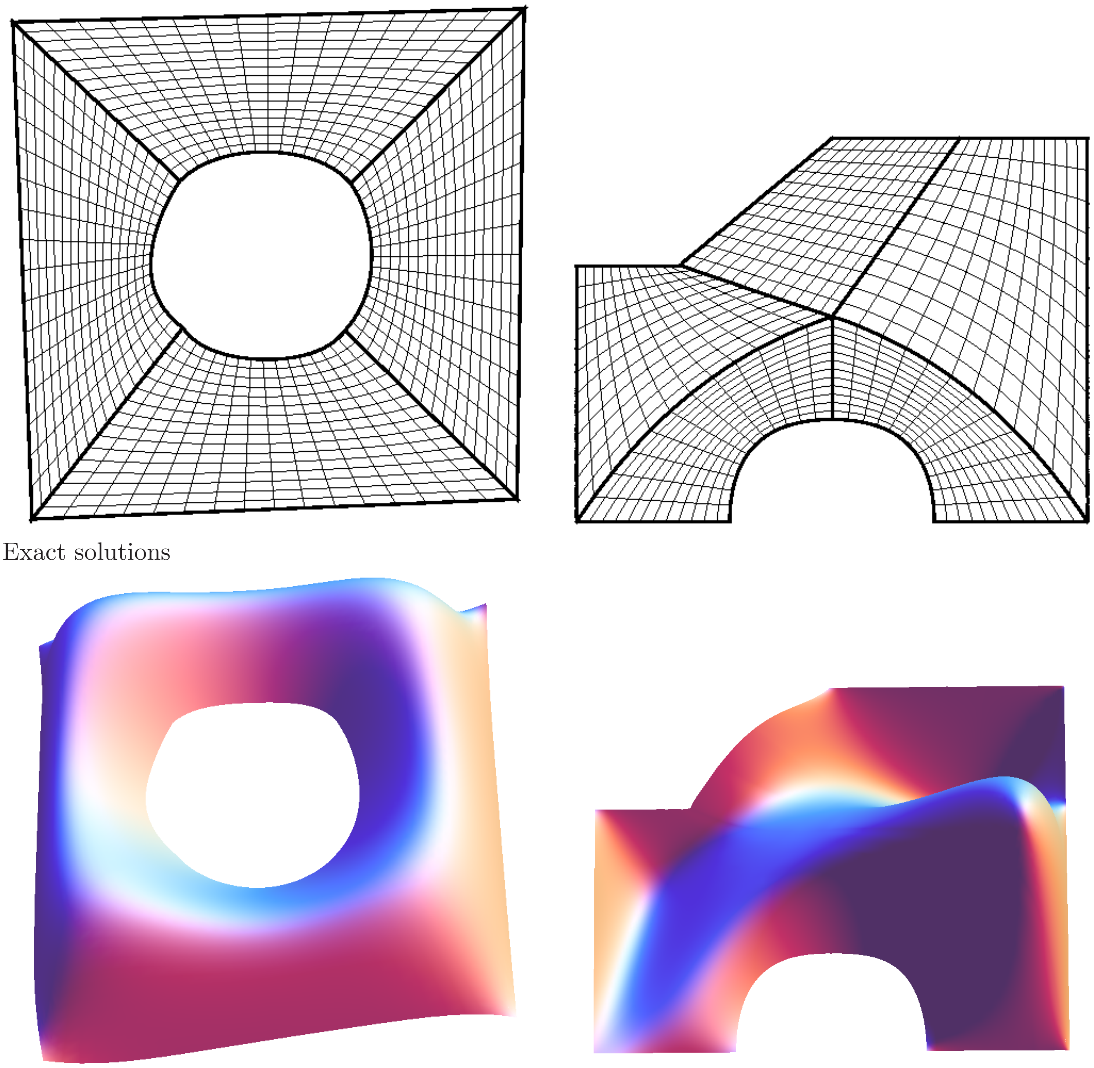

Relative H^i-errors, $i = 0, 1$

#ptchs	#fcts	rel. H^0-error	rel. H^1-error
64	644	1.009632e-04	4.041480e-04

#ptchs	#fcts	rel. H^0-error	rel. H^1-error
80	808	6.457694e-04	4.472207e-03

Figure 13: Two different computational domains (first row) with the exact solutions u for solving Poisson's equations (second row) and the relative H^i-errors, $i = 0, 1$ (third row).

Appendix A.1. Basis functions of type A, B and L

We present for both degrees $d \in \{3,4\}$ a possible choice of the $(2d+1)+(2d-4)k$ edge basis functions for a two patch domain Ω. As explained in Section 3.2, only Bézier coefficients $a_{\boldsymbol{i}}^{(\ell)}$ that correspond to the Bézier control points of the common interface of the two-patch domain or to the neighboring column of Bézier control points of the corresponding spline segments, can be non-zero for these functions. Consequently, their supports can be only contained in spline segments along the common interface, more precisely on one to four pairs of neighboring spline segments. Due to the size and location of these supports, we can classify the functions into different types (A, B, and L) with possible subtypes, see Fig. 4 and 5 and Table A.1. In the following, we specify simple explicit formulas for the non-zero values a_i of the corresponding Bézier coefficients of the different types of functions with respect to the local geometry given by the patch vertices $(0,0)$, $(0,2)/(0,3)$, (p_0,q_0), (p_1,q_1), (p_2,q_2), (p_3,q_3) visualized in Fig. 4 and Fig. 5 for $d=3$ and $d=4$, respectively. (Compare [10, Appendix] for $d=4$.) To present the formulas in a short and compact way, we will use the following auxiliary terms:

$$\alpha_{i,j} = p_i q_j - p_j q_i, \beta_{i,j} = p_j - p_i$$

and

$$\gamma_{i,j} = \alpha_{i,j} + \beta_{i,j}, \delta_{i,j} = \alpha_{i,j} + 2\beta_{i,j}, \varepsilon_{i,j} = \alpha_{i,j} + 3\beta_{i,j}, \eta_{i,j} = \alpha_{i,j} + 4\beta_{i,j}$$

for $i,j \in \{0,\ldots,3\}$ with $i<j$.

Table A.1: The different types of functions (A, B and L) for $d \in \{3,4\}$ possess supports that are contained in one to four pairs of neighboring spline segments along the common interface, see Fig. 4 and 5. Whereas the functions of type L are only defined on the lower and upper boundary of the common interface, the functions of type A and B are defined on each such possible pairs of neighboring spline segments along the common interface.

Type	# pairs of segments	location	subtypes	total number
		$d=3$		
A	3 pairs	on each such pairs	A	$k-1$
B	4 pairs	on each such pairs	B	$k-2$
L	1–2 pairs	both boundaries of common interface	L_1–L_5	10
		$d=4$		
A	2 pairs	on each such pairs	A_1–A_3	$3k$
B	3 pairs	on each such pairs	B	$k-1$
L	1–2 pairs	both boundaries of common interface	L_1–L_5	10

Basis functions of type A, B and L for $d=3$

- Type A:

$$a_6 = \frac{p_0}{3p_2+2p_3}, a_8 = \frac{p_2}{3p_2+2p_3}, a_9 = \frac{2p_0+p_1}{3p_2+2p_3}, a_{11} = \frac{2p_2+p_3}{3p_2+2p_3}, a_{12} = \frac{3p_0+2p_1}{3p_2+2p_3}, a_{14} = 1,$$
$$a_{15} = \frac{2p_0+3p_1}{3p_2+2p_3}, a_{17} = \frac{2p_2+3p_3}{3p_2+2p_3}, a_{18} = \frac{p_0+2p_1}{3p_2+2p_3}, a_{20} = \frac{p_2+2p_3}{3p_2+2p_3}, a_{21} = \frac{p_1}{3p_2+2p_3},$$
$$a_{23} = \frac{p_3}{3p_2+2p_3}.$$

- Type B:

$$a_8 = \frac{\alpha_{0,2}}{12p_0}, a_9 = \frac{\alpha_{0,1}}{16p_0}, a_{10} = \frac{1}{4}, a_{11} = \frac{3\alpha_{0,2}+\alpha_{0,3}}{16p_0}, a_{12} = \frac{\alpha_{0,1}}{8p_0}, a_{13} = \frac{1}{2}, a_{14} = \frac{7\alpha_{0,2}+3\alpha_{0,3}}{24p_0},$$
$$a_{15} = \frac{3\alpha_{0,3}p_0+\alpha_{0,3}p_1+8\alpha_{0,1}p_3}{48p_0p_3} + \frac{3\beta_{0,3}+\beta_{1,3}}{12p_3}, a_{16} = 1, a_{17} = \frac{3\alpha_{0,3}p_2+8\alpha_{0,2}p_3+9\alpha_{0,3}p_3}{48p_0p_3} + \frac{\beta_{2,3}}{12p_3},$$
$$a_{18} = \frac{\alpha_{0,3}(p_0+p_1)}{8p_0p_3} + \frac{\beta_{2,3}+\beta_{1,3}}{2p_3}, a_{19} = 1, a_{20} = \frac{\alpha_{0,3}(p_2+p_3)}{8p_0p_3} + \frac{\beta_{2,3}}{2p_3},$$
$$a_{21} = \frac{9\alpha_{0,3}p_0+11\alpha_{0,3}p_1-8\alpha_{0,1}p_3}{48p_0p_3} + \frac{9\beta_{0,3}+11\beta_{1,3}}{12p_3}, a_{22} = 1,$$
$$a_{23} = \frac{9\alpha_{0,3}p_2-8\alpha_{0,2}p_3+3\alpha_{0,3}p_3}{48p_0p_3} + \frac{3\beta_{2,3}}{4p_2}, a_{24} = \frac{3\eta_{0,3}+7\eta_{1,3}}{24p_3}, a_{25} = \frac{1}{2}, a_{26} = \frac{\eta_{2,3}}{8p_3},$$
$$a_{27} = \frac{\eta_{0,3}+3\eta_{1,3}}{16p_3}, a_{28} = \frac{1}{4}, a_{29} = \frac{\eta_{2,3}}{16p_3}, a_{30} = \frac{\eta_{1,3}}{12p_3}.$$

- Type L_1:

$$a_0 = \frac{2\gamma_{0,2}+\gamma_{0,3}}{2p_2+p_3}, a_1 = 1, a_2 = \frac{\gamma_{23}}{2p_2+p_3}, a_3 = \frac{4\gamma_{0,2}+2\gamma_{0,3}+2\gamma_{1,2}+\gamma_{1,3}}{18p_2+9p_3}.$$

- Type L_2:

$$a_1 = 1, a_2 = -\frac{\gamma_{0,2}}{p_0}, a_3 = -\frac{\gamma_{0,1}}{9p_0}, a_5 = -\frac{2\gamma_{0,2}+\gamma_{0,3}}{9p_0}.$$

- Type L_3:

$$a_2 = \frac{\alpha_{0,2}}{p_0}, a_3 = \frac{\delta_{0,2}+2\delta_{0,3}}{3p_2+6p_3} + \frac{\alpha_{0,1}}{9p_0}, a_4 = 1, a_5 = \frac{-2\alpha_{0,2}\beta_{2,3}+7\alpha_{0,3}p_2+2\alpha_{0,3}p_3}{9p_0(p_2+2p_3)} + \frac{4\beta_{2,3}}{3p_2+6p_3},$$
$$a_6 = \frac{11\delta_{0,2}+22\delta_{0,3}+4\delta_{1,2}+8\delta_{1,3}}{36p_2+72p_3}, a_7 = \frac{1}{2}, a_8 = \frac{\delta_{2,3}}{2p_2+4p_3}, a_9 = \frac{2\delta_{0,2}+4\delta_{0,3}+\delta_{1,2}+2\delta_{1,3}}{12p_2+24p_3},$$
$$a_{10} = \frac{1}{4}, a_{11} = \frac{\delta_{2,3}}{4p_2+8p_3}, a_{12} = \frac{\delta_{0,2}+2\delta_{0,3}+2\delta_{1,2}+4\delta_{1,3}}{36p2+72p3}.$$

- Type L_4:

$$a_3 = 1, a_5 = \frac{p_2}{p_0}, a_6 = \frac{11p_0+4p_1}{12p_0}, a_8 = \frac{11p_2+4p_3}{12p_0}, a_9 = \frac{2p_0+p_1}{4p_0}, a_{11} = \frac{2p_2+p_3}{4p_0}, a_{12} = \frac{p_0+2p_1}{12p_0},$$
$$a_{14} = \frac{p_2+2p_3}{12p_0}.$$

- Type L_5:

$$a_5 = \frac{2\alpha_{0,2}}{3p_0}, a_6 = \frac{2\alpha_{0,1}}{9p_0} + \frac{\varepsilon_{0,3}}{9p_3}, a_7 = 1, a_8 = \frac{2\alpha_{0,3}p_2+9\alpha_{0,2}p_3+4\alpha_{0,3}p_3}{18p_0p_3} + \frac{\beta_{2,3}}{3p_3},$$
$$a_9 = \frac{4\alpha_{0,3}p_0+2\alpha_{0,3}p_1+\alpha_{0,1}p_3}{18p_0p_3} + \frac{2\beta_{0,3}+\beta_{1,3}}{3p_3}, a_{10} = \frac{7}{6},$$
$$a_{11} = \frac{4\alpha_{0,3}p_2+2\alpha_{0,2}p_3+3\alpha_{0,3}p_3}{18p_0p_3} + \frac{2\beta_{2,3}}{3p_3}, a_{12} = \frac{3\varepsilon_{0,3}p_0+2\varepsilon_{0,3}p_1-\varepsilon_{0,1}p_3}{9p_0p_3} + \frac{3\beta_{0,1}}{9p_0}, a_{13} = \frac{4}{3},$$
$$a_{14} = \frac{6\alpha_{0,3}p_2-5\alpha_{0,2}p_3+2\alpha_{0,3}p_3}{18p_0p_3} + \frac{\beta_{2,3}}{p_3}, a_{15} = \frac{2\varepsilon_{0,3}+3\varepsilon_{1,3}}{9p_3}, a_{16} = \frac{2}{3}, a_{17} = \frac{2\varepsilon_{2,3}}{9p_3},$$
$$a_{18} = \frac{\varepsilon_{0,3}+2\varepsilon_{1,3}}{9p_3}, a_{19} = \frac{1}{3}, a_{20} = \frac{\varepsilon_{2,3}}{9p_3}, a_{21} = \frac{\varepsilon_{1,3}}{9p_3}.$$

Basis functions of type A, B and L for $d = 4$

- Type A_1:

$$a_6 = 1, a_8 = \frac{p_2}{p_0}, a_9 = 1 + \frac{3p_1}{4p_0}, a_{11} = \frac{4p_2+3p_3}{4p_0}, a_{12} = \frac{p_0+p_1}{2p_0}, a_{14} = \frac{p_2+p_3}{2p_0}, a_{15} = \frac{p_1}{4p_0},$$
$$a_{17} = \frac{p_3}{4p_0}.$$

- Type A_2:

  $a_8 = \frac{\alpha_{0,2}}{2p_0}, a_9 = \frac{3\alpha_{0,1}}{8p_0} + \frac{\delta_{0,3}}{8p_3}, a_{10} = 1, a_{11} = \frac{\alpha_{0,3}p_2+3\alpha_{0,2}p_3+3\alpha_{0,3}p_3}{8p_0p_3} + \frac{\beta_{2,3}}{4p_3},$
  $a_{12} = \frac{\alpha_{0,3}(p_0+p_1)}{4p_0p_3} + \frac{\beta_{0,3}+\beta_{1,3}}{2p_3}, a_{13} = 1, a_{14} = \frac{\alpha_{0,3}(p_2+p_3)}{4p_0p_3} + \frac{2\beta_{2,3}}{2p_3},$
  $a_{15} = \frac{3\alpha_{0,3}p_0+4\alpha_{0,3}p_1-3\alpha_{0,1}p_3}{8p_0p_3} + \frac{3\beta_{0,3}+4\beta_{1,3}}{4p_3}, a_{16} = 1, a_{17} = \frac{3\alpha_{0,3}p_2-3\alpha_{0,2}p_3+\alpha_{0,3}p_3}{8p_0p_3} + \frac{3\beta_{2,3}}{4p_3},$
  $a_{18} = \frac{\delta_{13}}{2p_3}.$

- Type A_3:

  $a_9 = \frac{p_0}{4p_3}, a_{11} = \frac{p_2}{4p_3}, a_{12} = \frac{p_0+p_1}{2p_3}, a_{14} = \frac{p_2+p_3}{2p_3}, a_{15} = \frac{3p_0+4p_1}{4p_3}, a_{17} = 1 + \frac{3p_2}{4p_3}, a_{18} = \frac{p_1}{p_3},$
  $a_{20} = 1.$

- Type B:

  $$\begin{aligned}&a_{11} = \frac{\alpha_{0,2}}{16p_0}, a_{12} = \frac{\alpha_{0,1}}{12p_0}, a_{13} = \frac{1}{4}, a_{14} = \frac{2\alpha_{0,2}+\alpha_{0,3}}{12p_0}, a_{15} = \frac{\alpha_{0,1}}{6p_0}, a_{16} = \frac{1}{2},\\ &a_{17} = \frac{13\alpha_{0,2}+8\alpha_{0,3}}{48p_0}, a_{18} = \frac{\varepsilon_{0,3}(2p_0+p_1)+\varepsilon_{0,1}p_3}{12p_0p_3} - \frac{\beta_{0,1}}{2p_0}, a_{19} = 1,\\ &a_{20} = \frac{2\varepsilon_{0,3}(p_2+p_3)-\varepsilon_{0,2}p_3}{12p_0p_3} - \frac{\beta_{0,2}+2\beta_{0,3}}{4p_0}, a_{21} = \frac{8\varepsilon_{0,3}+13\varepsilon_{1,3}}{48p_3}, a_{22} = \frac{1}{2}, a_{23} = \frac{\varepsilon_{2,3}}{6p_3},\\ &a_{24} = \frac{\varepsilon_{0,3}+2\varepsilon_{1,3}}{12p_3}, a_{25} = \frac{1}{4}, a_{26} = \frac{\varepsilon_{2,3}}{12p_3}, a_{27} = \frac{\varepsilon_{1,3}}{16p_3}.\end{aligned}$$

- Type L_1:

  $$a_0 = \frac{\gamma_{0,2}+\gamma_{0,3}}{p_2+p_3}, a_1 = 1, a_2 = \frac{\gamma_{2,3}}{p_2+p_3}, a_3 = \frac{\gamma_{0,2}+\gamma_{0,3}+\gamma_{1,2}+\gamma_{1,3}}{8p_2+8p_3}.$$

- Type L_2:

  $$a_1 = 1, a_2 = -\frac{\gamma_{0,2}}{p_0}, a_3 = -\frac{\gamma_{0,1}}{8p_0}, a_5 = -\frac{\gamma_{0,2}+\gamma_{0,3}}{8p_0}.$$

- Type L_3:

  $$\begin{aligned}&a_2 = \frac{\alpha_{0,2}}{p_0}, a_3 = \frac{6\gamma_{0,2}p_0+6\gamma_{0,3}p_0+\alpha_{0,1}(p2+p3)}{8p_0p_2+8p_0p_3}, a_4 = 1,\\ &a_5 = \frac{\alpha_{0,2}p_2+7\alpha_{0,3}p_2-5\alpha_{0,2}p_3+\alpha_{0,3}p_3}{8p_0p_2+8p_0p_3} + \frac{3\beta_{2,3}}{4p_2+4p_3}, a_6 = \frac{\gamma_{0,2}+\gamma_{0,3}+\gamma_{1,2}+\gamma_{1,3}}{4p_2+4p_3}.\end{aligned}$$

- Type L_4:

  $$a_3 = 1, a_5 = \frac{p_2}{p_0}, a_6 = \frac{p_0+p_1}{3p_0}, a_8 = \frac{p_2+p_3}{3p_0}.$$

- Type L_5:

  $a_5 = \frac{3\alpha_{0,2}}{4p_0}, a_6 = \frac{\alpha_{0,1}}{4p_0} + \frac{\delta_{0,3}}{4p_3}, a_7 = 1, a_8 = \frac{2p_0\beta_{2,3}+\alpha_{0,3}(p_2+p_3)}{4p_0p_3}, a_9 = \frac{4\delta_{0,3}+3\delta_{1,3}}{16p_3}, a_{10} = \frac{1}{2},$
  $a_{11} = \frac{\delta_{2,3}}{4p_3}, a_{12} = \frac{\delta_{0,3}+\delta_{1,3}}{8p_3}, a_{13} = \frac{1}{4}, a_{14} = \frac{\delta_{2,3}}{8p_3}, a_{15} = \frac{\delta_{1,3}}{16p_3}.$

Appendix A.2. Basis functions of type L^*

The functions of type L^* with respect to the local geometry visualized in Fig. 4 and Fig. 5 for the different degrees $d \in \{3,4\}$ can be obtained by linearly combining the functions of type L, i.e.

$$\mathrm{L}_i^* = \sum_{j=1}^{5} \mu_j^i \ \mathrm{L}_j, \ \ i \in \{1,\ldots,5\}.$$

The corresponding coefficients μ_j^i for the different degrees $d \in \{3,4\}$ are given below, where the auxiliary terms $\alpha_{i,j}$, $\beta_{i,j}$, $\gamma_{i,j}$, $\delta_{i,j}$ and $\varepsilon_{i,j}$ are the same as in Appendix A.1.

Basis functions of type L^* for $d = 3$

- type L_1^*:
$$\mu_1^1 = \frac{2p_2+p_3}{2\gamma_{0,2}+\gamma_{0,3}}, \mu_2^1 = \frac{\gamma_{0,3}p_2-\gamma_{0,2}p_3}{2\gamma_{0,2}^2+\gamma_{0,2}\gamma_{0,3}}, \mu_3^1 = 0, \mu_4^1 = -\frac{2\gamma_{0,2}+\gamma_{1,2}}{9\gamma_{0,2}},$$
$$\mu_5^1 = \frac{(\gamma_{0,3}+\gamma_{1,2}+\gamma_{0,2})p_2-\gamma_{0,2}\beta_{23}}{6\gamma_{0,2}\alpha_{0,2}}.$$

- type L_2^*:
$$\mu_1^2 = 0, \mu_2^2 = -\frac{p_0}{\gamma_{0,2}}, \mu_3^2 = 0, \mu_4^2 = -\frac{\gamma_{0,1}}{9\gamma_{0,2}}, \mu_5^2 = \frac{-2\gamma_{0,2}p_0-\gamma_{0,3}p_0+\gamma_{0,1}p_2}{6\gamma_{0,2}\alpha_{0,2}}.$$

- type L_3^*:
$$\mu_1^3 = 0, \mu_2^3 = 0, \mu_3^3 = 0, \mu_4^3 = 1, \mu_5^3 = -\frac{3p_2}{\alpha_{0,2}}.$$

- type L_4^*:
$$\mu_1^4 = 0, \mu_2^4 = \frac{\alpha_{0,2}}{\gamma_{0,2}}, \mu_3^4 = 1, \mu_4^4 = -\frac{3\gamma_{0,2}^2-(\gamma_{0,1}+\gamma_{1,2}-\gamma_{0,2})(p_2+2p_3)+\gamma_{0,2}(6\gamma_{0,3}+3\beta_{0,2}+6\beta_{0,3})}{9\gamma_{0,2}(p_2+2p_3)},$$
$$\mu_5^4 = \frac{3\gamma_{0,2}^2-\gamma_{0,3}\beta_{0,2}-(\gamma_{0,1}+\gamma_{1,2}-\gamma_{0,2})p_2+\gamma_{0,2}(3\beta_{0,2}+\beta_{0,3})}{6\gamma_{0,2}\alpha_{0,2}}.$$

- type L_5^*:
$$\mu_1^5 = 0, \mu_2^5 = 0, \mu_3^5 = 0, \mu_4^5 = 0, \mu_5^5 = \frac{3p_0}{2\alpha_{0,2}}.$$

Basis functions of type L^* for $d = 4$

- type L_1^*:
$$\mu_1^1 = \frac{p_2+p_3}{\gamma_{0,2}+\gamma_{0,3}}, \mu_2^1 = \frac{\gamma_{0,3}p_2-\gamma_{0,2}p_3}{\gamma_{0,2}^2+\gamma_{0,2}\gamma_{0,3}}, \mu_3^1 = 0, \mu_4^1 = -\frac{\gamma_{0,2}+\gamma_{1,2}}{8\gamma_{0,2}}, \mu_5^1 = \frac{(\gamma_{0,3}+\gamma_{1,2})p_2-\gamma_{0,2}\beta_{2,3}}{6\gamma_{0,2}\alpha_{0,2}}.$$

- type L_2^*:
$$\mu_1^2 = 0, \mu_2^2 = -\frac{p_0}{\gamma_{0,2}}, \mu_3^2 = 0, \mu_4^2 = -\frac{\gamma_{0,1}}{8\gamma_{0,2}}, \mu_5^2 = -\frac{\gamma_{0,2}p_0+\gamma_{0,3}p_0-\gamma_{0,1}p_2}{6\gamma_{0,2}\alpha_{0,2}}.$$

- type L_3^*:
$$\mu_1^3 = 0, \mu_2^3 = 0, \mu_3^3 = 0, \mu_4^3 = 1, \mu_5^3 = -\frac{4p_2}{3\alpha_{0,2}}.$$

- type L_4^*:
$$\mu_1^4 = 0, \mu_2^4 = \frac{\alpha_{0,2}}{\gamma_{0,2}}, \mu_3^4 = 1, \mu_4^4 = -\frac{6\gamma_{0,2}^2-(\gamma_{0,1}+\gamma_{1,2}-\gamma_{0,2})(p_2+p_3)+6\gamma_{0,2}\gamma_{0,3}}{8\gamma_{0,2}(p_2+p_3)},$$
$$\mu_5^4 = \frac{6\gamma_{0,2}^2-\gamma_{0,3}\beta_{0,2}-(\gamma_{0,1}+\gamma_{1,2}-\gamma_{0,2})p_2+\gamma_{0,2}\beta_{0,3}}{6\gamma_{0,2}\alpha_{0,2}}.$$

- type L_5^*:
$$\mu_1^5 = 0, \mu_2^5 = 0, \mu_3^5 = 0, \mu_4^5 = 0, \mu_5^5 = \frac{4p_0}{3\alpha_{0,2}}.$$

Appendix A.3. Basis functions of type Y

The functions of type Y with respect to the local geometry visualized in Fig. 4 and Fig. 5 for $d = 3$ and $d = 4$, respectively, can be obtained by linearly combining the functions of type L^*, i.e.

$$\mathrm{Y}_i = \sum_{j=1}^{5} \mu_j^i \, \mathrm{L}_j^*, \; i \in \{1, \ldots, 5\},$$

where the coefficients μ_j^i for the different functions of type Y.i for the degrees $d \in \{3, 4\}$ are given as follows:

- type Y_1:
$$\mu_1^1 = 1, \mu_2^1 = 1, \mu_3^1 = 0, \mu_4^1 = 1, \mu_5^1 = 0.$$

- type Y_2:
$$\mu_1^2 = \tfrac{p_0 \cos\varphi + q_0 \sin\varphi}{d}, \mu_2^2 = \tfrac{p_2 \cos\varphi + q_2 \sin\varphi}{d}, \mu_3^2 = 0, \mu_4^2 = \tfrac{\sin\varphi}{d}, \mu_5^2 = 0.$$

- type Y_3:
$$\mu_1^3 = \tfrac{p_0 \cos\varphi - q_0 \sin\varphi}{d}, \mu_2^3 = \tfrac{p_2 \cos\varphi + q_2 \sin\varphi}{d}, \mu_3^3 = 0, \mu_4^3 = \tfrac{\cos\varphi}{d}, \mu_5^3 = 0.$$

- type Y_4:
$$\mu_1^4 = 0, \mu_2^4 = 0, \mu_3^4 = 1, \mu_4^4 = 0, \mu_5^4 = 0.$$

- type Y_5:
$$\mu_1^5 = 0, \mu_2^5 = 0, \mu_3^5 = 0, \mu_4^5 = 0, \mu_5^5 = 1.$$

Note, that φ is the angle between the vector $(1, 0)$ and the directional vector of the common interface of the two patches with respect to global coordinates. In addition, the corresponding boundary vertex $\boldsymbol{v}_0$ of the common edge for the construction of these functions corresponds to the point $(0, 0)$ of the local geometry visualized in Fig. 4 and Fig. 5 for $d = 3$ and $d = 4$, respectively.

References

[1] M. Bercovier and T. Matskewich. Smooth Bézier surfaces over arbitrary quadrilateral meshes. Technical Report 1412.1125, arXiv.org, 2014.

[2] E. Brivadis, A. Buffa, B. Wohlmuth, and L. Wunderlich. Isogeometric mortar methods. *Comp. Methods Appl. Mech. Engrg.*, 284:292–319, 2015.

[3] F. Buchegger, B. Jüttler, and A. Mantzaflaris. Adaptively refined multi-patch B-splines with enhanced smoothness. *Applied Mathematics and Computation*, 2015. in press.

[4] J. A. Cottrell, T.J.R. Hughes, and Y. Bazilevs. *Isogeometric Analysis: Toward Integration of CAD and FEA.* John Wiley & Sons, Chichester, England, 2009.

[5] G. Farin. *Curves and surfaces for computer-aided geometric design*. Academic Press, 1997.

[6] D. Groisser and J. Peters. Matched G^k-constructions always yield C^k-continuous isogeometric elements. *Computer Aided Geometric Design*, 34:67 – 72, 2015.

[7] Y. Guo and M. Ruess. Nitsche's method for a coupling of isogeometric thin shells and blended shell structures. *Comp. Methods Appl. Mech. Engrg.*, 284:881–905, 2015.

[8] J. Hoschek and D. Lasser. *Fundamentals of computer aided geometric design*. A K Peters Ltd., Wellesley, MA, 1993.

[9] T. J. R. Hughes, J. A. Cottrell, and Y. Bazilevs. Isogeometric analysis: CAD, finite elements, NURBS, exact geometry and mesh refinement. *Comput. Methods Appl. Mech. Engrg.*, 194(39-41):4135–4195, 2005.

[10] M. Kapl, V. Vitrih, B. Jüttler, and K. Birner. Isogeometric analysis with geometrically continuous functions on two-patch geometries. *Comput. Math. Appl.*, 2015. in press.

[11] K. Karčiauskas, T. Nguyen, and J. Peters. Generalizing bicubic splines for modelling and iga with irregular layout. 2015. submitted.

[12] S. Kleiss, C. Pechstein, B. Jüttler, and S. Tomar. IETI – isogeometric tearing and interconnecting. *Computer Methods in Applied Mechanics and Engineering*, 247-248:201–215, 2012.

[13] U. Langer, A. Mantzaflaris, S.E. Moore, and I. Toulopoulos. Multipatch discontinuous Galerkin isogeometric analysis. Technical Report 18, NFN Geometry + Simulation, 2014. available at *www.gs.jku.at*.

[14] T. Nguyen, K. Karčiauskas, and J. Peters. A comparative study of several classical, discrete differential and isogeometric methods for solving poisson's equation on the disk. *Axioms*, 3(2):280–299, 2014.

[15] T. Nguyen, K. Karčiauskas, and J. Peters. C^1 finite elements on non-tensor-product 2d and 3d manifolds. 2015. submitted.

[16] V.P. Nguyen, P. Kerfriden, M. Brino, S.P.A. Bordas, and E. Bonisoli. Nitsche's method for two and three dimensional NURBS patch coupling. *Comput. Mech.*, 53(6):1163–1182, 2014.

[17] J. Peters. Geometric continuity. In *Handbook of computer aided geometric design*, pages 193–227. North-Holland, Amsterdam, 2002.

[18] M.A. Scott, R.N. Simpson, J.A. Evans, S. Lipton, S.P.A. Bordas, T.J.R. Hughes, and T.W. Sederberg. Isogeometric boundary element analysis using unstructured t-splines. *Comp. Methods Appl. Mech. Engrg.*, 254:197 – 221, 2013.

[19] M.A. Scott, D.C. Thomas, and E.J. Evans. Isogeometric spline forests. *Comp. Methods Appl. Mech. Engrg.*, 269:222–264, 2014.

[20] Th.W. Sederberg, D.L. Cardon, G.Th. Finnigan, N.S. North, J. Zheng, and T. Lyche. T-spline simplification and local refinement. *ACM Trans. Graph.*, 23(3):276–283, 2004.

[21] Th.W. Sederberg, J. Zheng, A. Bakenov, and A. Nasri. T-splines and T-nurccs. *ACM Trans. Graph.*, 22(3):477–484, 2003.